

**Design and Analysis of Internal 20 K Helium Gas
Purification System for the kW Class Helium
Refrigerator/Liquefier**

A Thesis Submitted in Partial Fulfillment of the Requirements for

The Degree of

Master of Technology

In

Mechanical Engineering

By

**Adarsh Kumar Behera
212ME5403**



Department of Mechanical Engineering

National Institute of Technology

Rourkela

2014

**Design and analysis of internal 20K helium gas
purification System for the kW class Helium
Refrigerator/Liquefier**



**A Thesis Submitted in Partial Fulfillment of the Requirements for
The Degree of**

Master of Technology

In

Mechanical Engineering

By

**Adarsh Kumar Behera
212ME5403**

Under the supervision of

Internal Supervisor:

Mr. A. K. Sahu

Scientist / Engineer – SF

Division Head, Large Cryogenic Plant & Cryosystem,

Institute for Plasma Research,

Bhat, Gandhinagar-38242

College Guide:

PROF. R.K Sahoo

Department of Mechanical Engineering

National Institute of Technology

Rourkela-769008

CERTIFICATE

This is to certify that the dissertation, entitled
**“Design and Analysis of Internal 20 K Helium Gas Purification System for the
kW Class Helium Refrigerator/Liquefier”**

is a bonafide work done by

Adarsh Kumar Behera

*Under my close guidance and supervision in the Large Cryogenic Plant and Cryosystem Group
of*

Institute for Plasma Research, Gandhinagar, Gujarat

*for the partial fulfillment of the award for the degree of Master of Technology in Mechanical
Engineering with Specialization in Cryogenic and Vacuum Technology at*

National Institute of Technology, Rourkela.

*The work presented here, to the best of my knowledge, has not been submitted to any university
for the award of similar degree.*

GUIDE:

Mr. A. K. Sahu

Scientist / Engineer – SF

Division Head Large Cryogenic Plant and Cryosystem

Institute for Plasma Research

Gandhinagar – 382 428

Gujarat, India



Certificate of Approval

This is to certify that the thesis entitled “**Design and Analysis of Internal 20 K Helium gas Purification system for kW class Helium Refrigerator/ Liquefier**”, submitted to the National Institute of Technology, Rourkela, by **Adarsh Kumar Behera**, Roll No. **212ME5403** for the award of the Degree of **Master of Technology in Mechanical Engineering** with specialization “**Cryogenic and Vacuum Technology**”, is a record of bonafide research work carried out by him under my supervision and guidance. The results presented in this thesis have not been, to the best of my knowledge, submitted to any other University or Institute for the award of any degree or diploma.

The thesis in my opinion has reached the standards fulfilling the requirement for the award of the degree of **Master of Technology** in accordance with regulations of the institute.

Mr. A. K. Sahu
Scientist/Engineer-SF, Division Head,
Large Cryogenic plant and Cryosystem,
Institute for plasma Research,
Gandhinagar, Gujarat

Prof. R.K. Sahoo
Department of Mechanical Engineering
National Institute of Technology,
Rourkela

Contents

CERTIFICATES.....	i
CONTENTS.....	iii
ACKNOWLEDGEMENT.....	v
ABSTRACT.....	vi
LIST OFFIGURES.....	viii
LIST OF TABLES.....	viii
INTRODUCTION.....	1
LITERATURE REVIEW.....	4
2.1Overview of Previous Research Works:.....	4
2.2Basic Definitions Of The Present Research Work As Follows:.....	5
2.3 ADSORPTION EQUILLIBRIUM.....	6
2.3.1 ADSORPTION ISOTHERMS:.....	7
2.3.2 MODELLING OF DIFFERENT ISOTHERMS:.....	8
2.4 CONCENTRATION PATTERNS IN FIXED BED PROCESS.....	12
2.5 BREAK THROUGH CURVES:.....	13
2.6 MASS TRANSFER ZONE:.....	13
2.7 ANALYTICAL MODELS TO PREDICT BREAK THROUGH CURVES:.....	14
2.7.1 Axial Dispersion Model:.....	15
2.7.2 THE ROSEN MODEL:.....	15
2.7.3Effective Diffusivity:.....	16
2.8 ADSORBENT SELECTION:.....	18
2.9 ACTIVATED CARBON DEFINITION & PREPARATION:.....	19
2.10 PRESSURE DROP ACROSS THE FIXED BED:.....	20
2.11 PRESSURE DROP IN THE FILTER CATRIDGE:.....	21
PROCESS PARAMETERS & METHODOLOGY.....	23
3.1 MASS OF CHARCOAL NEEDED FOR PURIFIER BED.....	25
3.1.1ADSORBENT FOR SATURATION ZONE:.....	25
3.2 ADSORBENT FOR MTZ:.....	27
3.21 Optimization of the pressure Drop:.....	28

3.3 HENRY CONSTANT (K_H).....	29
3.3.1 Effective Diffusivity Calculation:	31
3.4 MTZ using Axial Dispersion Model:.....	31
3.5 MTZ using DIMENSIONLESS ROSEN MODEL:	32
3.6 FINAL DIMENSIONS OF THE BED AND PRESSURE DROP:.....	34
3.7 STRESS ANALYSIS OF THE DESIGNED PURIFIER BED IN ANSYS:	35
PRESSURE DROP CALCULATION FOR FILTER CATRIDGE.....	36
Results and Discussion	41
5.1 DIMENSIONS OF THE PURIFIER BED:	41
5.2 PRESSURE DROP IN PURIFIER BED:	42
5.3 Mass Transfer Zone.....	43
5.3.1 Independency of Henry constant for calculation for the MTZ:	43
5.4 MTZ Variation with changing Different Parameters for ROSEN MODEL:	45
5.5 PRESSURE DROP VARIATIONS IN THE SCREEN.....	47
Conclusion.....	49
References:	50

ACKNOWLEDGEMENT

I am extremely thankful to **Mr A.K SAHU** Scientist / Engineer – SF ,Division Head Large Cryogenic Plant and Cryosystem, Institute for Plasma Research, for his erudite suggestions, perceptive remarks, wondrous guidance and affection. He has helped me from prologue to epilogue. I remain ever grateful to him for his valuable suggestions for the accomplishment of this thesis work.

With respectable regards and immense pleasure I take it as a privilege to express my profound sense of gratitude and indebtedness to my supervisor **Prof.R .K SAHOO**, Professor, Department of Mechanical Engineering, NIT Rourkela, Rourkela, for his encouragement, guidance and great support during the project work. He was always motivated and shares his expertise during the whole course of project work. I owe a deep debt of gratitude to him and remain grateful to him.

My special thanks to **Mr.N.C Gupta** Scientist / Engineer – SE, Large Cryogenic Plant and Cryosystem, Institute for Plasma Research and **Mr. Hardik Vyas** Project Engineer, Institute for Plasma Research for their support throughout the project work.

I like to thank my friends especially **Mr. Punit Kar and Mr. Divyang Vohra** who worked with me in every difficulties that I faced. Their encouragement and efforts were the tremendous sources of inspiration .

I shall be failing in my duty, if I don't express my thanks to **NIT ROURKELA** for providing me the financial help in the form of stipend and also encouragement to complete the study successfully.

ABSTRACT

The Helium refrigerator/Liquefier (HRL) is normally operated with helium gas having purity better than 99.999% by volume which is equivalent to having 10PPM (parts per million) impure gas in helium gas. Although sufficient precautions and impurity removal procedures are used, still, in the process of gas transfer or due to some other processes before reaching to liquefaction, impurity level sometimes can go as high as 500 PPM averaging to about 100 PPM. These impurities mainly consists of gases present in the air, like $N_2, O_2, Ar, H_2, H_2O, CO, CO_2$ and the traces of Ne. Hydrocarbons of the lubricating oil can also be sources of H_2 . These gases condense at significantly higher temperature compared to LHe (4.5K). If such high level of impurity enters the process equipment placed inside the cold box of HRL, then it can condense and choke the pipelines and the valves leading to large pressure drop and inefficient liquefaction process. Sometimes condensed and choked impurity can destroy the blades of turbines of the HRL. Hence to be on safer side generally, internal purifiers are placed at two temperature levels inside the cold box to take care the operational problem due to impurities. One is at 80K to remove N_2, O_2, Ar . And another one is at 20K to remove H_2 . This project is about the design and analysis of 20K purification system to be used for the planned indigenous helium plant of equivalent cooling capacity ~2 kW at 4.5 K. The impurity level of H_2 in helium gas stream is expected to about 10 to 100 PPM. Activated charcoals are to be used to adsorb impure gases from cold helium gas at 20K and 80K at ~14 bar. The nominal flow rate of helium, entering the 20 K purifier system, is 100 gm/sec. These single bed type purifier will be designed to condense the amount of impurities that are expected to reach the cold box in the operation period of one week after which it can be purged and made ready for next operation. The size of LHe Dewar is 1500 Ltr storage capacity. The maximum quantity of impurity to be removed from the helium gas will depend on the equivalent quantity of helium gas required to make 1500 Ltrs of LHe in operation. This is the major quantity of helium need to be drawn from the storage tank and which can bring impurities. Besides this, some extra helium gas will be required to draw which will be circulating and filling the helium plant components during operation. As this quantity is insignificant, the impurity for this is taken care by considering design margin in the purifier. At the outlet of the 20K purifier, the total impurity should be 1PPM. At the downstream of the adsorber bed, fine filters of 30 micron pore size should be placed to trap the charcoal dust

which can come sometime through the helium stream. This purifier will be a part of the indigenous helium development project. In this context, this work also involves the manufacturing, assembly, test, repair aspect of these purifiers

LIST OF FIGURES:

Figure 1 Process Flow Diagram of Indigenous helium refrigerator/liquefier plant being developed at IPR 2	
Figure 2 Different Types of Adsorption Isotherms.....	7
Figure 3 Classification of Isotherms	8
Figure 4 Monolayer & Multilayer Adsorption Phenomenon	10
Figure 5 concentration Patterns in Fixed Bed Process	13
Figure 6 Break through Curves in Fixed bed	13
Figure 7 Surface Area of Adsorbent in Increased Magnification	18
Figure 8 Pore size distribution of Various Adsorbents.....	19
Figure 9 Flow chart & Methodology	24
Figure 10 Characteristic Curve of Hydrogen at 20K.....	26
Figure 11 Hydrogen Adsorption Isotherm developed from D-R equation	27
Figure 12 Adsorption Isotherm correlation for Henry constant	30
Figure 13 Break Through Curve for Axial Dispersion Model.....	32
Figure 14 Break through Curve using Rosen Model	33
Figure 15 structural analysis of the designed purifier bed in Ansys	35
Figure 16 Pressure Drop vs. Screen Width for Filter cartridge	38
Figure 17 3-D drawing Outer Casing of the Filter Cartridge 2-.....	38
Figure 18 2-D drawing of inner design of the filter cartridge.....	39
Figure 19 2-D Drawing of 20K Purifier Bed	41
Figure 20 L/d vs. Pressure Drop varying the Void Porosity.....	42
Figure 21 L/d vs. Pressure Drop varying the Particle diameter keeping constant void porosity.....	42
Figure 22 MTZ vs. KH for Rosen Model.....	43
Figure 23 MTZ vs. KH for (KH=7210)	44
Figure 24 MTZ vs. KH for (KH=2500)	44
Figure 25 Time vs Concentration ratio with changing Interstitial Velocity for Rosen Model.....	45
Figure 26 Time vs Concentration ratio with changing the Particle diameter	46
Figure 27 Particle Diameter(meters) vs. MTZ % in Rosen Model	46
Figure 28 Pressure Drop Variation with porosity for Filter Screen.....	47
Figure 29 Pressure Drop Variation with Screen Width	47

LIST OF TABLES

Table 1 PROCESS PARAMETERS for Purifier Bed.....	23
Table 2 Process Parameters for Stress Analysis of Purifier bed	35
Table 3 PROCESS PARAMETERS FOR FILTER CARTRIDGE Design	36
Table 4 Internal design and dimensions of the Filter cartridge.....	39
Table 5 Independency of Henry constant	43
Table 6 variation of MTZ with interstitial velocity	45

INTRODUCTION

Helium, is the second most abundant element available in the universe but in earth's atmosphere only 0.0005% of helium is found. This very less amount of helium is in gaseous form and lost to the outer space continuously. Inside the earth's crust, helium is produced by the alpha decay of radioactive elements. In the alpha decay of the radioactive elements, when the alpha particle occupies two electrons from the surrounding media it becomes a helium atom. This is how trace amount of helium is formed in the crust of the earth.

Helium has some exceptionally unique properties like low boiling point, low density, low solubility, high thermal conductivity. Due to these above mentioned unique properties helium is found very much useful in space research, quantum mechanics, leak detection, controlled atmosphere, cryogenics industry and superconductivity applications.

1.1 LIQUID HELIUM:

Kamerlingh Onnes on 10th July 1908 produced 60 cubic centimeters of liquid helium. He used liquid air to produce liquid hydrogen and used liquid hydrogen to jacket the liquefaction apparatus to produce liquid helium. The boiling point of liquid helium was found 4.2 K. Kamerlingh Onnes received noble prize for this remarkable breakthrough.

Helium is having a boiling temperature which is close to 0 K. The critical temperature and pressure of helium is 5.2 K and 2.3 bars respectively. At 2.17 K, in the liquid helium, there occurs a discontinuity in the heat capacities and the density drops so that fraction of the liquid becomes zero viscosity and called as SUPERFLUID helium and this point is also called as lambda point. Super fluidity is due to the fraction of helium atoms condensed in to the lowest possible energy state which leads to changes in the properties of the liquid helium and called "LAMBDA POINT" of liquid helium. At the superfluid condition, a zero viscosity fluid which can move through any pore of the material, at this condition the conductivity of the helium becomes 30 times the conductivity of copper. These are the properties that make liquid helium very important in the study of superconductivity and for the applications of superconducting magnets.

1.2 HELIUM LIQUEFIER AT IPR:

The process instrumentation diagram of the proposed indigenous HRL is given below.

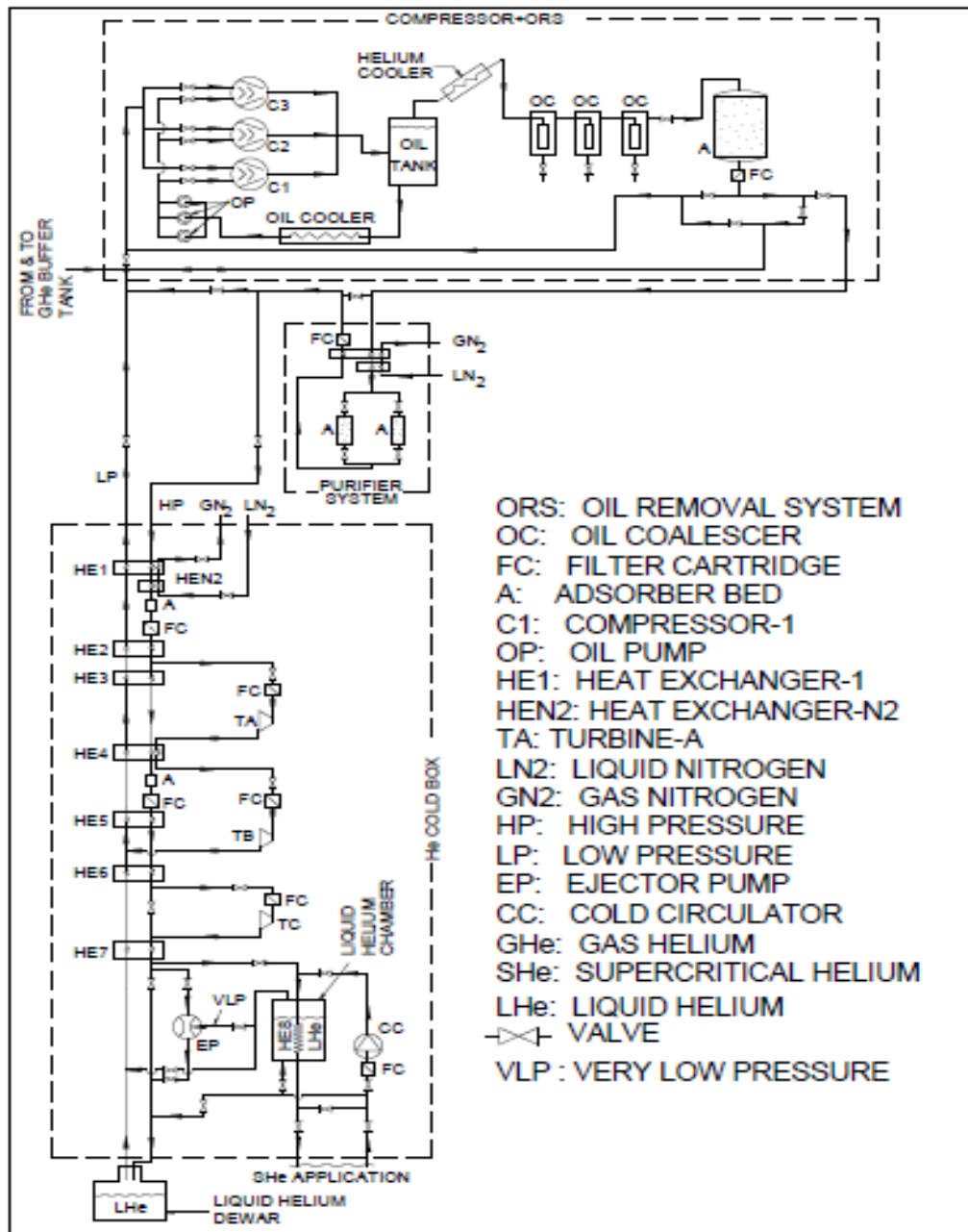


Figure 1 Process Flow Diagram of Indigenous helium refrigerator/liquefier plant being developed at IPR

1.3 NEED FOR PURIFYING HELIUM:

The helium stream before entering into the cold box of the HRL passes through an external purification unit. Though sufficient precaution is taken, still, in the process of gas transfer and some other processes the helium stream gets contaminated and impurity level sometimes goes up to 500 PPM. Though the impurity is in PPM range it can cause damage to cold box by condensing or choking in the pipe lines that leads to damage the turbine blades and inefficient liquefaction. These impurities mainly consists of gases present in the air, like $N_2, O_2, Ar, H_2, H_2O, CO, CO_2$ and the traces of Ne. Hydrocarbons of the lubricating oil can also be sources of H_2 .

These contaminants comes due to various reasons like when the isolated equipment bled down to atmospheric pressure, the barometric pressure changes throughout the day which causes changes in pressure in piping. The bed is not purged of contamination during installation. During maintenance oil in the pipes exposed to air has an affinity to attract contamination. The make up of lost helium also brings inbuilt impurity.

The cold box of the HRL contains two purification units placed at 80K and 20K. The 80K purification unit is to purify impurities like N_2, O_2, Ar as these impurities condense below the boiling point temperature of liquid nitrogen. The 20K purifier unit is to purify H_2 and traces of Neon present. The source of Ne is atmospheric air and the source of H_2 is natural gas from where helium is extracted. The compressor lubricating oil in the helium plant can be a source of H_2 as at certain points of the circuit, the temperature of helium can go up to 100 K.

As the amount of neon present is very less and its boiling point temperature is higher than 20K it is of less concern for purification. This 20K purifier mainly deals with removing Hydrogen impurity. The mechanism used in purification is physical adsorption.

LITERATURE REVIEW

2.1 Overview of Previous Research Works:

Purer et al. (1965) conducted experiments for ultra-purification of helium and used U.S. Bureau of Mines Grade-A helium with Neon as major impurity. They run the setup for three different adsorbents like charcoal, molecular sieve and silica gel for temperature range varying from 30K to 175K and found that charcoal 10 times more effective than molecular sieve and 70 times more effective than silica gel. In the final test runs they used charcoal and reported ultrapure helium containing less than 2ppb of Neon and no detectable traces of other impurities. They also reported that adsorptive capacity of charcoal for Neon at 77K is low as compared to that of 35K.[1]

Kidnay and Hiza (1967) performed some experiments at 76K on Helium, Hydrogen and Neon at developed adsorption isotherms at pressure range varying from 0 to 100 atmospheres. They have used desorption technique to measure the adsorption isotherm. They reported that for hydrogen adsorption the amount adsorbed is high for charcoal than zeolite. Also they have obtained isotherms from mathematical correlations developed by Dubinin and compared with the experimental data, the agreement between the experimental and the predicted values are excellent. [2]

Kidnay et al. (1968) reported the adsorption isotherms of nitrogen, methane, hydrogen and their mixtures on charcoal at 76K. It was reported that in the binary adsorption isotherm, nitrogen and methane showed decrease in capacity with pressure while hydrogen showed increase in capacity with pressure. The ternary isotherms were calculated using the relation developed by Kidnay and Myers, and it was assumed that Hydrogen was the carrier gas for methane and nitrogen. The calculated values in the ternary isotherm exhibited close proximity with experimental values. [3]

Wang and Johnson (1998) formulated methods for calculating adsorption isotherms of Hydrogen on graphite and carbon slit pores by combining Grand Monte Carlo simulations with

path integral method. They have compared the simulated data with the experimental data found that the agreement between these two is very good. They have also shown the comparison between the experimental and simulated data at 20K for Para Hydrogen and it was observed that the simulation data lie below the predicted data.[4]

2.2 Basic Definitions Of The Present Research Work As Follows:

ADSORPTION:

Adsorption has been defined as operation that uses surface forces on solid bodies called adsorbents to achieve the concentration of volatile materials. Adsorption differs from absorption, in which a fluid (the adsorbate) permeates or diffuses into the liquid or solid (the absorbent). Adsorption is a surface-based process while absorption involves the whole volume of the material. The adsorption process is broadly classified into two processes i.e. Physical adsorption and chemical adsorption. The mechanism of adsorption is significantly different in these two processes.

2.2.1 PHYSICAL ADSORPTION (PHYSISORPTION):

The forces involved in physical adsorption are intermolecular force of attraction like (Vander wall's force, Hydrogen bonding). It does not change the structure of the species involved in molecular level.

Physical adsorption is of reversible type and no surface reaction takes place. It is observed under low temperature and heat of adsorption is low. The adsorption can be mono-molecular layer or multi-molecular layer.

2.2.2 CHEMICAL ADSORPTION (CHEMISORPTION):

The forces involved in chemisorption differ from physisorption that here the forces involved are valence forces which lead to formation of new compound. It changes the structure of the species in molecular level and heat of adsorption is high. In chemisorption surface reactions like dissociation, reconstruction, catalysis may take place. These processes are irreversible in nature and follow mono-molecular layer formation.

2.2.3 CRYOGENIC ADSORPTION MECHANISM:

Cryogenic adsorption is based on the physical adsorption, using different adsorbents. These adsorbents have a porous and divided material, with a specific area as high as 500 to 2500 m²/g. The physical adsorption is a reversible process (adsorption / desorption) and an exothermic process, where the adsorption heat is similar to the latent heat. The adsorption often consists of three processes, i.e. the outside diffusion, the inside diffusion and the intramural adhesion. These physical processes occur quickly, and the phase balance among different components will be achieved instantly. According to adsorption thermodynamics, if the adsorbent and the adsorbate are both at uniform temperature and pressure, the adsorbate quantity is dominated by the adsorbed gas pressure and the adsorption equilibrium temperature. Adsorbate gases flows through the adsorbent bed, the adsorbent first forms a mass transfer area. After this mass transfer area is formed, as long as the gas flow rate is uniform, its length also increases uniformly along the flow direction when more impurities are adsorbed. In the dynamic adsorption process, the adsorbent's bed is divided into three sections, the saturated adsorbent zone, the adsorption mass transfer zone and the clean adsorbent zone. The adsorbent used here is activated charcoal.

2.3 ADSORPTION EQUILLIBRIUM:

Adsorption occurs when the adsorbate comes in contact with the adsorbent layer, after some time both the adsorbate and adsorbent reaches to an equilibrium condition with respect to the temperature (T), pressure (P), and the equilibrium amount adsorbed (W) in gm/gm of adsorbent. These three variables describes the adsorption phenomenon by keeping one constant at a time and rest of the two as a function of each other.

When temperature is kept constant and the equilibrium amount adsorbed is expressed as a function of pressure only it is called as adsorption isotherm i.e. $W=f(P)$

When pressure is kept constant and the equilibrium amount adsorbed is expressed as a function of temperature it is called adsorption isobar $W=f(T)$, likewise keeping the amount adsorbed constant and expressing pressure as a function of temperature it is called as isostere.

While designing adsorption systems the most important parameter is the adsorption isotherm. It is used to determine the amount of adsorbent needed to for the equilibrium amount to be adsorbed and also determines the dimensions of the system and time of operation.[5,19]

2.3.1 ADSORPTION ISOTHERMS:

The adsorption isotherms are the equilibrium relationship between the concentration in the fluid phase and concentration of adsorbent particles in a given temperature. For gases the concentration is usually given in mole percent or as a partial pressure. For liquids the concentration is expressed in terms of mass units such as parts per million.

These isotherms can be favorable, unfavorable, linear, may be irreversible type. The linear isotherm goes through the origin and the amount adsorbed is proportional to the concentration in the fluid. Isotherms that are convex upwards are called favorable, because a relatively high solid loading can be obtained at low concentration in the fluid. Isotherms that are concave upward are unfavorable because low solid loading is obtained. The limiting case of a very favorable isotherm is irreversible adsorption, where the amount adsorbed is independent of concentration down to very low value. In adsorption the dynamic equilibrium should be maintained i.e. the rate of adsorption is equal to rate of desorption. [5,19]

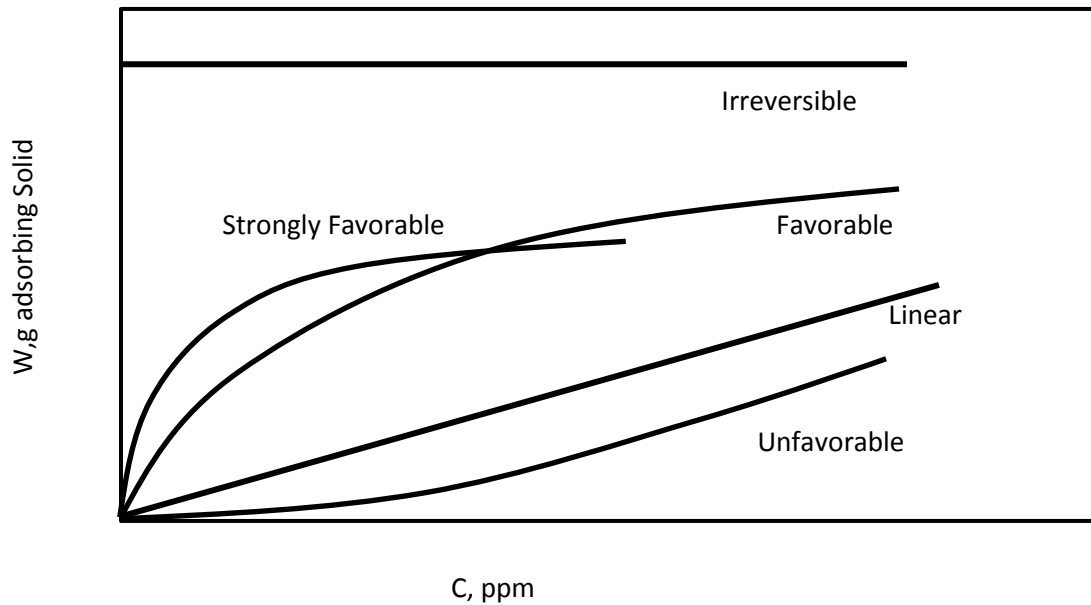


Figure 2 Different Types of Adsorption Isotherms

(Courtesy: unit operations of chemical engineering 5th edition Ed, McCabe, Smith)

According to IUPAC isotherms are classified into six types. These isotherms are shown in the figure below.

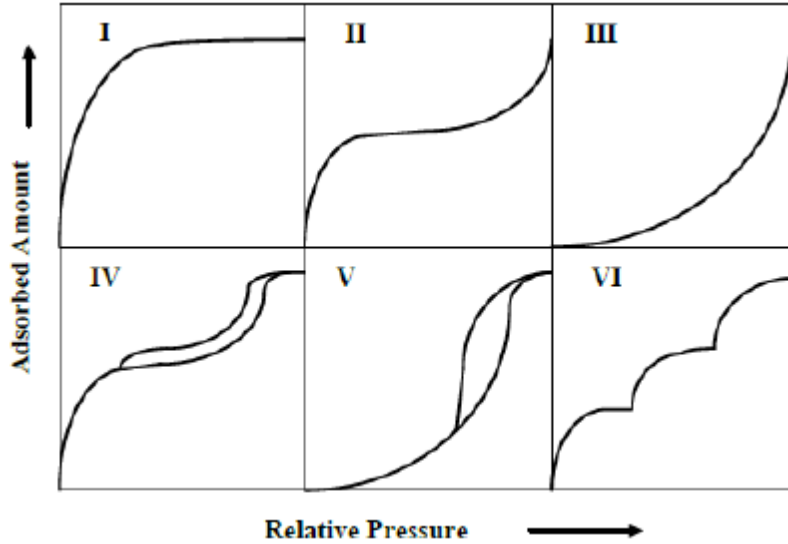


Figure 3 Classification of Isotherms

(Courtesy: IUPAC Classification of Isotherms)

I- Monolayer adsorption

II- Multilayer adsorption,

III-Island or droplet nucleation necessary for adsorption

IV- Pore filling, followed by outer-surface adsorption

V- Pore filling with nucleation (like III), followed by outer surface adsorption

VI- Discrete steps adsorption may be due to formation of multilayer in different ranges of micro-pores

2.3.2 MODELLING OF DIFFERENT ISOTHERMS:

2.3.2.1 LANGMUIR MODEL:

This model is described by **Irving Langmuir** (1916) for gases adsorbed into solids. It is used to quantify the amount of adsorbate adsorbed into the adsorbent is a function of partial pressure at that temperature.

Assumption made by Langmuir :

1. The adsorbent surface consists of a certain number of active sites (proportional to the surface area), at each of which only one molecule may be adsorbed.
2. No lateral interaction between the molecules so the heat of adsorption is constant and independent of coverage.

3. The adsorbed molecule remains at the sight of the adsorption until it is desorbed.
4. At maximum adsorption only a single layer of molecule is formed i.e. molecules don't deposit on one another.

The equation of the model is given by

$$W = W_{\max} \left(\frac{Kc}{1 + Kc} \right)$$

Where W= adsorbate loading

c= concentration of fluid

K=adsorption constant

The Langmuir adsorption isotherm is based on assumptions that uniform surface, which is not valid as multilayer adsorption can also happen but the relation works well for the gases that are weakly adsorbed.[5]

2.3.2.2 BET MODEL:

This model is proposed by **Brunauer et al.** (1938). This is based on the multilayer adsorption model. It also assumes that there is equal energy of adsorption for each layer except for the first layer. This model describes many experimental phenomenon which are not described by Langmuir [6]

Assumptions of BET model:

1. Multi-layer adsorption. The Vander walls force of adsorption is stronger in the case of solid and gas phase than gas phase. It means that the heat of adsorption is higher in the 1st layer than the 2nd and subsequent layers.
2. There is no lateral interaction as in case of Langmuir.
3. The adsorption surface is homogeneous.

The adsorption of the second and subsequent layers occurs with a heat of adsorption equal to the heat of condensation of the adsorbate.

The equation of this model is given by

$$\frac{V}{M_a} = \frac{V_m Z \frac{P}{P_{sat}}}{\left[\left(1 - \frac{P}{P_{sat}} \right) \left(1 + (z-1) \frac{P}{P_{sat}} \right) \right]}$$

Where V = volume of gas adsorbed

M_a = mass of adsorbent

V_m = volume of gas per unit mass of adsorbent required to form a monomolecular layer over the entire adsorbent surface

P = partial pressure of gas being adsorbed

P_{sat} = saturation pressure of the gas being adsorbed at the temperature of the adsorbent

Z = it is a function of energy of adsorption and temperature of adsorbent

$Z = \exp(\theta_a/T)$

The values of θ_a and V_m are different for various gases and adsorbents.

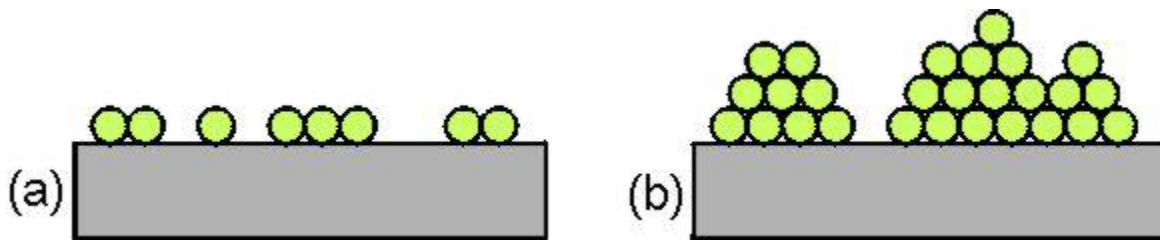


Figure 4 Monolayer & Multilayer Adsorption Phenomenon

(a) Mono-layer adsorption-Langmuir isotherm

(b) Multilayer adsorption-BET isotherm

DRAWBACKS:

1. Langmuir model is applied only to mono-molecular adsorption.
2. BET theory is derived on the assumption that the pressure ratio should vary in the range 0.05 to 0.3, which can't be used in case very low partial pressures.

2.3.2.3 POLANYI POTENTIAL THEORY :

The major drawback in Langmuir model is the assumption of monomolecular adsorption. And BET theory multilayer adsorption is based on the assumption of higher pressure ratio. **Polanyi Potential Theory** is based on the multi molecular pore filling which is a fitting theory for adsorption on highly porous materials like activated carbon and zeolites.

Polanyi's theory assumed that the force field can be represented by the equipotential contours above the surface, and the space between each set of equipotential surfaces corresponds to a definite adsorbed volume.[7]

This volume adsorbed (W) is a function of the adsorption potential (ϵ)

$$W = f(\epsilon) \quad (1)$$

This function remains unspecified but is characteristic of particular gas-solid system and hence referred to as characteristic curve. The characteristic curve is independent of temperature as adsorption potential expresses the work of temperature independent dispersion forces.

The adsorption potential is equal to work required to remove one molecule from its location in adsorbed phase to gas phase and can be related to pressure. The adsorption potential represents the molar free energy change with the change in vapour pressure from that over pure liquid phase P_0 to equilibrium pressure P at a given coverage of adsorbent surface.

The mathematical formula can be written as

$$\varepsilon = RT \ln \left(\frac{P_0}{P} \right) \quad (2)$$

2.3.2.4 DUBININ-RADUSHKEVICH (D-R) EQUATION:

The **Dubinin-Radushkevich** (1947) equation is the adaptation of the Polanyi potential theory. The D-R equation emphasizes on the micro pore volume filling of the adsorbent material rather than layer formation on the wall of the adsorbent material. According to this theory, adsorbent materials like activated carbon, silica gel, zeolites contain varieties of pore sizes but it is the micropore volume that determines the extent of adsorption.[8]

The development of D-R equation two important parameters are taken one is adsorption potential and other is the volume of the micropore. In this theory Dubinin expressed the adsorption potential as the negative of the differential free energy of adsorption. Another parameter θ is introduced such a way that

$$\theta = \frac{W}{W_0} \quad (3)$$

W_0 = total volume of the micropore

W =volume that has been filled when the relative pressure is P/P_0

Here in this equation θ is a function of adsorption potential ε in such a manner that

$$\theta = f \left(\frac{\varepsilon}{E} \right) \quad (4)$$

$E = E_0 \beta$

E = characteristic adsorption energy

E_0 = Adsorption energy of the reference vapour

β = affinity coefficients, similarity coefficients or relative differential molar works of adsorption

Assuming the pore size distribution is Gaussian, Dubinin and Radushkevitch found out the expression

$$\frac{w}{w_0} = \exp \left[- \left(\frac{\varepsilon}{E} \right)^2 \right] \quad (5)$$

Where $\varepsilon = RT \ln \left(\frac{P_0}{P} \right)$

And $E = E_0 \beta$

Dubinin-Astakhov (D-A) equation is the more generalized form of D-R equation, is expressed as [9]

$$\frac{w}{w_0} = \exp \left[- \left(\frac{\varepsilon}{E} \right)^{n_1} \right] \quad (6)$$

Here $n =$ Heterogeneity factor depends upon the surface

$n = 2$ for Carbonaceous materials

$= 4-6$ for Zeolites

2.4 CONCENTRATION PATTERNS IN FIXED BED PROCESS:

In the fixed bed adsorption system, the concentrations in the fluid phase change with time and position of the bed. At the inlet of the bed when the impure stream comes in contact with the adsorbent layer, the adsorbent layer contains no impurity but as the time increases and adsorption takes place the impurity concentration in the fluid phase drops to zero before the end of the bed reached.

The concentration pattern is shown below. At time t_1 , C/C_0 is the concentration relative to the feed and as the time progresses the solid adsorbent at the inlet gets saturated and wave front travels further in the bed. At t_2 the concentration gradient takes the S-shape. The region where most of the mass transfer takes place is called MASS TRANSFER ZONE and the maximum outlet concentration ratio is taken as 0.95 to 0.05 which indicates that the bed is saturated [5].

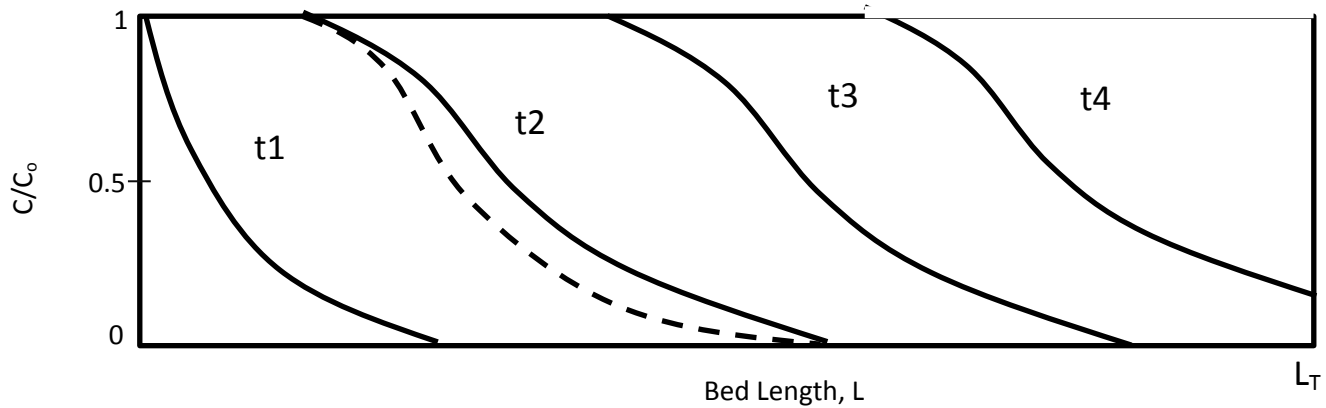


Figure 5 concentration Patterns in Fixed Bed Process

(Courtesy: unit operation in chemical engineering McCabe, Smith)

2.5 BREAK THROUGH CURVES:

In very few beds the profile of the beds can be assumed internally, though these profiles can be predicted and used in calculating the curve of concentration v/s time for fluid leaving the bed. The curve shown below is a breakthrough curve, at time t_1 and t_2 the exit concentration is practically zero. When the concentration reaches a limiting permissible value the flow is stopped or the stream is changed to another bed. The break point is even taken as 0.05 or 0.1. If the flow continued flowing beyond the break point the impurity concentration will rise.

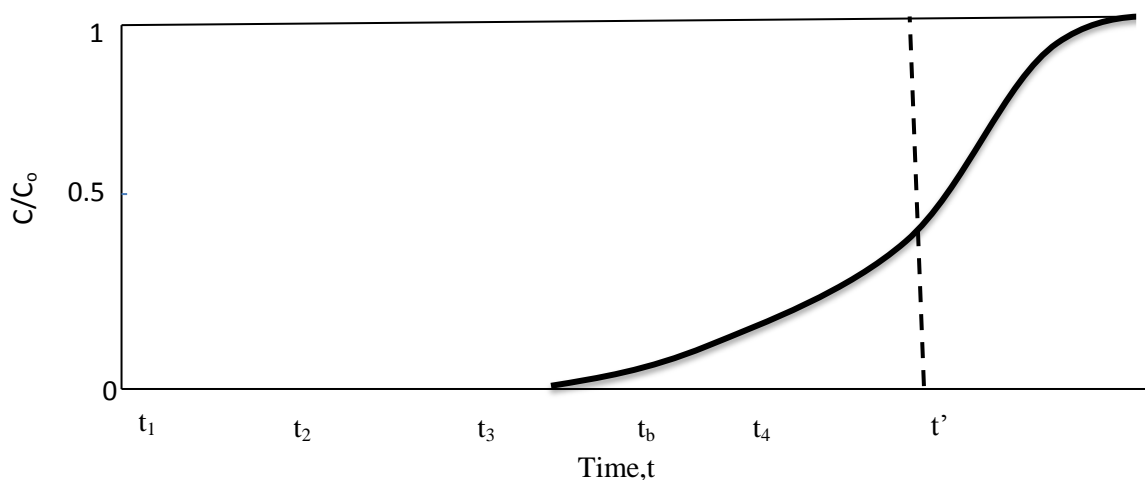


Figure 6 Break through Curves in Fixed bed

(Courtesy: unit operation in chemical engineering McCabe, Smith)

Here in the above mentioned curve t_b is the Break through time and t^* is time when outlet concentration reaches 50% of inlet.

2.6 MASS TRANSFER ZONE:

The adsorption process in a packed bed does not occur in the whole bed length during the operation. In other words a certain length of bed, called mass transfer zone (MTZ), is involved in the adsorption process and it starts moving along the bed, from the inlet point to the outlet point during the operation time. Within the MTZ, the degree of saturation with adsorbate varies from 100% to zero and the fluid concentration varies from the inlet concentration to zero. As the activated carbon in this zone reaches its equilibrium capacity, or in other words becomes

exhausted, the MTZ will travel further through the carbon bed. Thus a section of exhausted carbon bed is left behind the MTZ and a section of fresh carbon particles is in front of the leading edge of the MTZ. When the front edge of the MTZ reaches the end point of the bed, the breakthrough point occurs.

The length of the MTZ is a function of the influent flow rate and the rate of adsorption. If the length of the bed is less than the length of the MTZ, the effluent concentration does not equal zero from the beginning of the process. Besides, the MTZ formation is not instantaneous. It needs a certain time called formation time. Thus if the time of MTZ formation is less than the residence time of the bed, the effluent concentration would again be nonzero at the beginning of the process. Therefore the length and velocity of MTZ are two important factors of adsorption bed design. Minimizing the length of the MTZ increases the capacity of the bed, and this can be used to achieve a predetermined the objective.

2.7 ANALYTICAL MODELS TO PREDICT BREAK THROUGH CURVES:

Break through curves are nothing but graphical representation of concentration vs. time. As time increases the adsorbent in the bed starts to saturate and after a certain instant there will be rise in impurity in the outlet from the bed. The time in this rise in the impurity can be noted as break through time and as the bed saturating the time instant is called as saturation time. The length of bed within this time difference is called 'Length of MTZ' or 'Length of Unused Bed'. The length of MTZ is to be found out to get the dimensions of the adsorber bed. In order to find out we need to find out MTZ length we need to find out the Break through curves. It can be found out analytically and experimentally.

There are various analytical models proposed to predict the breaks through curves, out of them two very successful models are stated below. [10,19]

1. Axial Dispersion Model
2. Rosen Model

2.7.1 Axial Dispersion Model:

The axial dispersion model is based on the concept that the concentration front is dispersed by both hydrodynamic (hydrodynamic) and kinetic (finite transport rates) factors. The equation for the axial dispersion model is given by [5,10,11]

$$\frac{c}{c_0} = \frac{1}{2} \left[1 - \frac{\text{erf}\left(1 - \frac{t}{t'}\right)}{2\left(\frac{D_z t}{u L t'}\right)^{0.5}} \right] \quad (7)$$

$$t' = \frac{L}{u} \left[1 + K_H \frac{(1-\varepsilon)}{\varepsilon} \right] \quad (8)$$

$$D_z = De \left(\gamma_1 + \frac{\gamma_2 (ReSc)}{\varepsilon} \right) \quad (9)$$

$$\gamma_1 = 0.45 + 0.55\varepsilon \quad (10)$$

$$\gamma_2 = 0.5 \left(1 + \frac{13\gamma_1 \varepsilon}{ReSc} \right)^{-1} \quad (11)$$

t = time

C=Outlet concentration

C₀=Inlet concentration

D_z=axial dispersion coefficient

u = interstitial velocity

L = length of total bed

K_H=dimensionless Henry constant

ε= void porosity

De= effective diffusivity

D_m=molecular diffusivity

D_k=Knudsen's Diffusivity

r=pore radius

$$Sc = \frac{v}{De}$$

2.7.2 THE ROSEN MODEL:

The Rosen Model, developed by Rosen helps in finding analytical solutions to adsorption problems. The basic assumptions for this model are stated below.[5,10,11,19]

1. No Axial dispersion
2. Isothermal conditions and linear isotherm
3. Constant flow velocity
4. Constant effective diffusivity

The dimensionless form of Rosen Model is given below.

$$\frac{c}{c_0} = \frac{1}{2} \left[1 + \operatorname{erf} \left\{ \frac{\left(\frac{3U}{2V} \right) - 1}{2 \left(\frac{1+5\nu}{5V} \right)^{0.5}} \right\} \right] \quad (12)$$

$$U = 2De \frac{\left(t - \frac{L}{u} \right)}{Rp^2} \quad (13)$$

$$V = \frac{(3DeK_H L)}{uRp^2} \left(\frac{\varepsilon}{1-\varepsilon} \right) \quad (14)$$

$$\nu = \frac{DeK}{kRp} \quad (15)$$

C=Outlet concentration

C₀=Inlet concentration

U=dimensionless contact parameter

V=dimensionless bed length parameter

ν= dimensionless film resistance

R_p=pellet radius

K_H=Henry constant

2.7.3 Effective Diffusivity:

Effective diffusivity is a function of molecular diffusivity and Knudsen diffusivity.[12,19]

$$\frac{1}{D_e} = \frac{1}{D_m} + \frac{1}{D_k} \quad (16)$$

$$D_m = \frac{0.0018583T^{3/2}}{P\sigma_{12}^2\Omega_{12}} \left(\frac{1}{M_A} + \frac{1}{M_B} \right)^{0.5} \quad (17)$$

$$D_k = 9700r \left(\frac{T}{M} \right)^{1/2} \quad (18)$$

D_e = effective diffusivity

D_m =molecular diffusivity

D_k =Knudsen's Diffusivity

P =pressure, atm

T =temperature in K

Ω_D =collision integral= $f(kT/\epsilon_{AB})$

k =Boltzmann constant

ϵ =Lennard-Jones force constant for common gases

$\epsilon_{AB}=(\epsilon_A * \epsilon_B)^{0.5}$

$\sigma_{AB}=(\sigma_A + \sigma_B)/2$ =effective collision diameter, \AA^0

2.8 ADSORBENT SELECTION:

Adsorbents adsorb the impurity from the effluent stream. These are the solid surfaces upon which the impurities get collected over. These adsorbent should have some unique properties like listed below.

1. High surface area
2. High internal volume
3. Good mechanical properties

There are different types of adsorbents available

- .activated carbon
- .silica gel
- .zeolites
- .molecular sieves
- .activated alumina

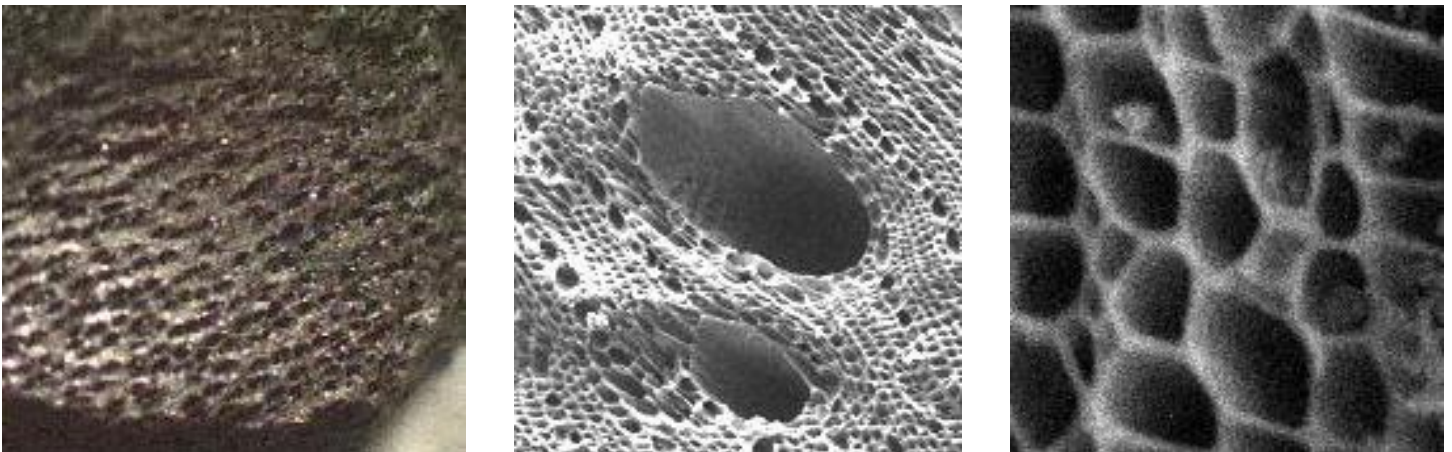


Figure 7 Surface Area of Adsorbent in Increased Magnification

Out of all the above adsorbent materials activated charcoal is selected due to its high surface area good mechanical strength, high iodine number, high pore volume, abrasion number, bulk density. Activated charcoal has a very wide range of surface area varying from 500-1600 m²/gram.[11]

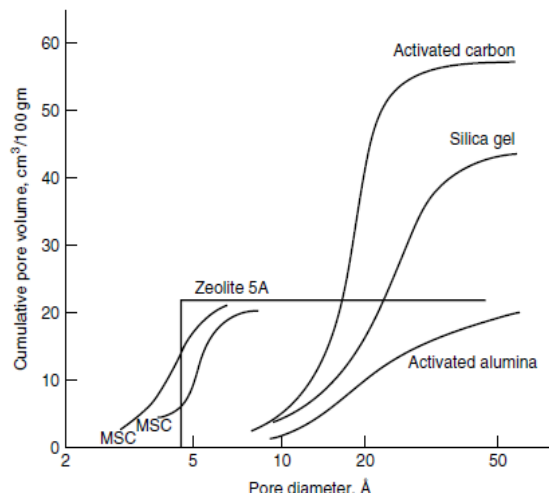


Figure 8 Pore size distribution of Various Adsorbents

Pore-size distributions for activated carbon, silica gel, activated alumina, two molecular sieve carbons and zeolite 5A (Courtesy: Yang R.T., Adsorbents fundamentals and applications,).

As per IUPAC classification of pore sizes

Micropore < 2nm diameter

Mesopores = 2nm to 50 nm diameter

Macropore > 50 nm

A comparison shown between zeolite and activated carbon and its shown that activated carbon has higher potential in low temperature adsorption

2.9 ACTIVATED CARBON DEFINITION & PREPARATION:

Activated carbon is an adsorbent having very high porosity with a complex structure of graphite like sheets called “Basal Planes”. These basal planes are joined by random cross linking. In graphite layers the basal planes stacked in a very orderly manner unlike the activated carbon. Due to the random cross linking and randomized bonding of the basal planes, activated carbon results in a highly porous structure.

The porosity and enormous internal surface area makes activated carbon useful in various adsorption applications.

Usually Activated Carbons are prepared by steam treatment or by chemical treatment. Steam treatment being more common and easy to handle is used widely. Steam activation usually involves two steps.

1. Carbonization

2. Activation

In carbonization the raw material used such as coal, wood based coal into a highly porous and low volatile material. Carbonization is done at high temperature and oxygen lean environment.

The next step in the operation is activation. In activation process carbon is made to react with the steam to form carbon monoxide and hydrogen gas and resulted in a highly porous structure.



In some activation units the carbon monoxide and hydrogen gas may be burned to produce heat to maintain the activation temperature. The resulting pores are aligned along adjacent basal planes and are therefore slit shaped. Initially micropores are formed. Prolonged activation results in micropores enlarging to Mesopores and eventually to macropores [13].

2.10 PRESSURE DROP ACROSS THE FIXED BED:

While designing a packed bed adsorption system the pressure drop across the bed plays an important role in determining the dimensions of the bed. Pressure drop largely depends on the size of the charcoal used i.e. the particle diameter of the charcoal granule, void fraction of the bed, superficial velocity. In cryogenic applications especially inside the cold box, pressure drop needs to be optimized and it should be maintained within the stipulated range or it will lead to inefficient liquefaction.

In a packed bed system in order to calculate pressure drop the actual flow channel is replaced with parallel cylindrical conduits of constant cross section. Pressure drop occurs due to inertial and viscous effects. When the Reynolds no is high the effects are inertial or else viscous.[14]

1. Rate of fluid flow

2. Viscosity and density of the fluid

3. Closeness and orientation of packing

4. Size shape and surface of the particles

To calculate the pressure losses, we rely on a friction factor correlation attributed to Ergun. Ergun equation describes flow in both laminar and turbulent regimes. To calculate the pressure drop, the ERGUN model is adopted.

$$F_P = \left(\frac{\Delta P}{L}\right) \left(\frac{D_P}{\rho U_0^2}\right) \left(\frac{\varepsilon^3}{1-\varepsilon}\right) \quad (19)$$

$$Re = \frac{\rho U_0 D_P}{(1-\varepsilon)\mu} \quad (20)$$

F_P = friction factor for the Packed bed

L = the height of the bed

μ =the fluid viscosity

ε =void porosity

U_0 = the fluid superficial velocity

D_P =the particle diameter

ΔP = Pressure drop

2.11 PRESSURE DROP IN THE FILTER CARTRIDGE:

Filter cartridge is a circular tube like structure containing screens for purifying the helium stream. After the Helium stream is purified in the adsorption due to high pressure and very low temperature some of the charcoal granule gets dusted with size varying from 10 to 30 micron which comes in the high pressure line leaving the purifier bed. Charcoal dusts coming in the high pressure line can cause blockages in the pipelines leading to huge pressure drop and inefficient liquefaction. To contain these small particles metallic wire mesh screens of 30micron size used with no of screens varying from 10 to 50.[15]

In case of designing of the filter cartridge ERGUN equation is used

The expression of ERGUN equation for the calculation of pressure drop across a metallic screen is given by.

$$Re_{Erg} = \frac{\rho V_s^6}{\mu} \quad (21)$$

$$fr = \frac{\alpha}{Re} + \beta \quad (22)$$

$$\Delta P = \frac{fr\rho V_s^2 B(1-\varepsilon)\alpha}{6\varepsilon^3} \quad (23)$$

Taking $\varepsilon=0.3$

$$\alpha=150(1-\varepsilon)$$

$$\beta=1.75$$

$$a=4/d$$

d=wire diameter of the screen

PROCESS PARAMETERS & METHODOLOGY

As per design, the peak liquefaction rate of the helium plant is ~500lits/hr. As this is an experimental plant, the non-peak operation is expected more frequently and hence here, liquefaction rate of 100 ltr/hr is considered for design of the purification system. If purifier is designed for lower liquefaction rate, then it will work as overdesign for higher liquefaction rate.

Table 1 PROCESS PARAMETERS for Purifier Bed

LHe Dewar volume	1500 ltrs
Operating Pressure	14bar
Operating temperature	20K
Mass flow rate of Helium stream	0.1 kg/sec
Designed Impurity level inlet	100 PPM
Volume flow rate of Helium Stream(14 bar and 20K)	0.003 m ³ /sec
Micropore volume (Shell based)	0.4 cm ³ /gm
Maximum Pressure Drop	50 mbar
Charcoal density	550 kg/m ³
Void fraction	0.48-0.6
Particle diameter of charcoal	0.002m

Flow Chart for CALCULATION METHODOLOGY:

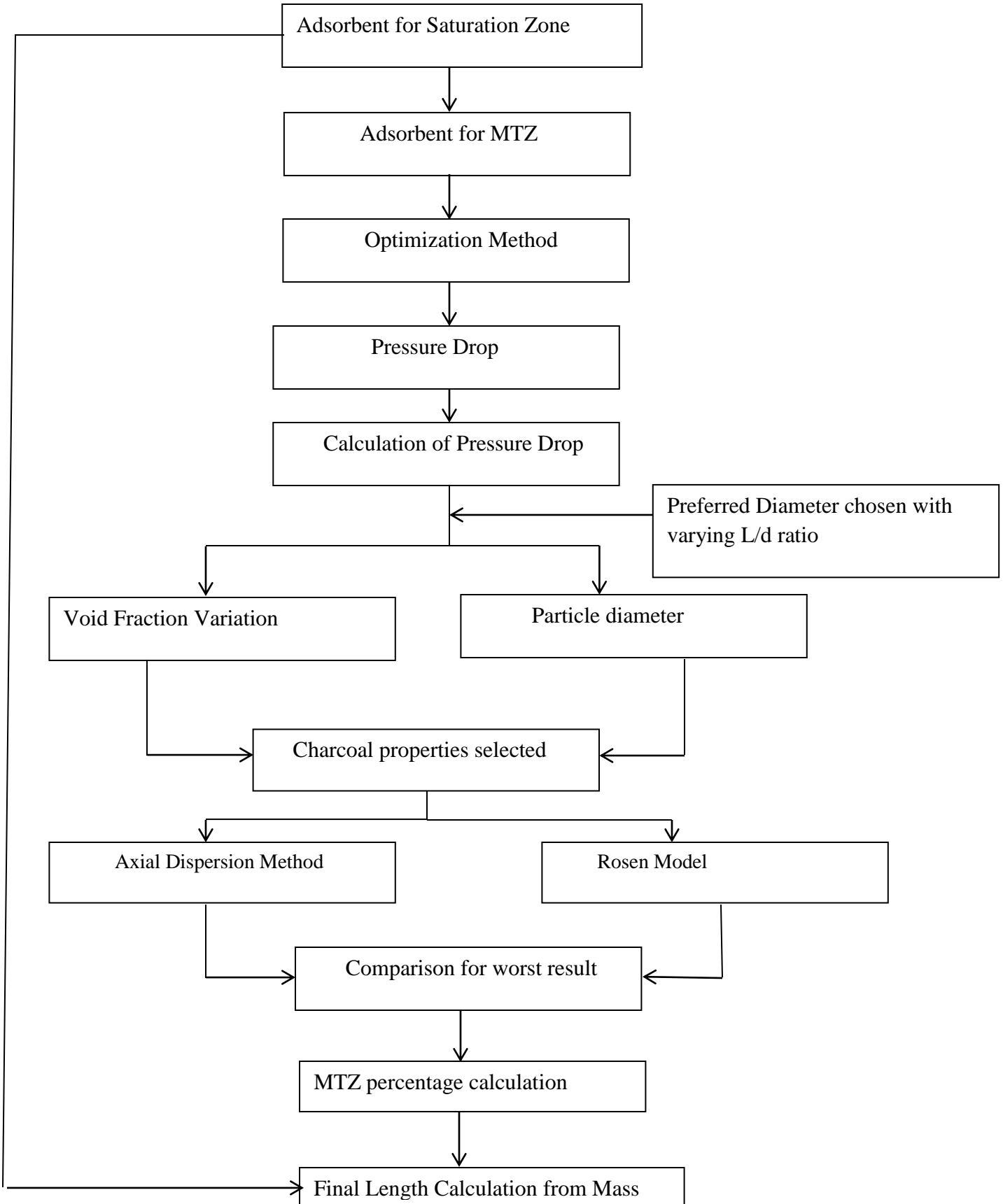


Figure 9 Flow chart & Methodology

3.1 MASS OF CHARCOAL NEEDED FOR PURIFIER BED:

3.1.1 ADSORBENT FOR SATURATION ZONE:

ASSUMPTIONS [16]

1. Micropore Volume filling based on D-R equation
2. Activated carbon used: Coconut Shell Based Charcoal
3. For Coconut shell based charcoal the micropore volume (W_0) = 0.0000004 m³/gm
4. Adsorption energy for reference vapour Benzene (E_0) = 23.5Kj/mole

Calculations:

Mass flow rate of Helium = 0.1 kg/sec

Equivalent amount of Helium at STP = 0.176 kg/m³

Equivalent volume of Helium (V_{He}) = 0.1/0.176

$$= 0.56 \text{ Nm}^3/\text{sec}$$

Designed Hydrogen impurity amount 100PPM for 100 liters/hr liquid production and 15 hours of operation

$$= 0.56 * 100 * 10^{-6} * 3600 * 15$$

$$= 3 \text{ Nm}^3$$

Equivalent Mass of Hydrogen Impurity (M_{eq}) at STP is found to be

$$= 3 \text{ Nm}^3 * \text{density of Hydrogen at STP}$$

$$= 3 * 0.088$$

$$= 0.264 \text{ kg}$$

$$\text{Adsorption Potential } \varepsilon = RT \ln \left(\frac{P_0}{P} \right)$$

$$= 1.097588 \text{ KJ/mole}$$

Affinity coefficient for Hydrogen (β) = 0.311

Bulk Density of Activated carbon = 550 kg/m³

Adsorption Capacity (W_0) from the D-R equation as stated below

$$W = W_0 \exp \left[- \left(\frac{\varepsilon}{E_0 \beta} \right)^2 \right]$$

$W = 0.028447116$ gm of H₂ adsorbed / gram of activated carbon

The Mass of activated carbon (M_{ad}) needed to adsorb 100 PPM Of impurity

$$= M_{eq} / W$$

$$= 0.264 / 0.028447116 = 9.28 \text{ Kg}$$

The amount of adsorbent needed to adsorb impurity of 100 PPM is found to be 9.28 kg, rounding it to 10kg.

Characteristic Curve for Hydrogen:

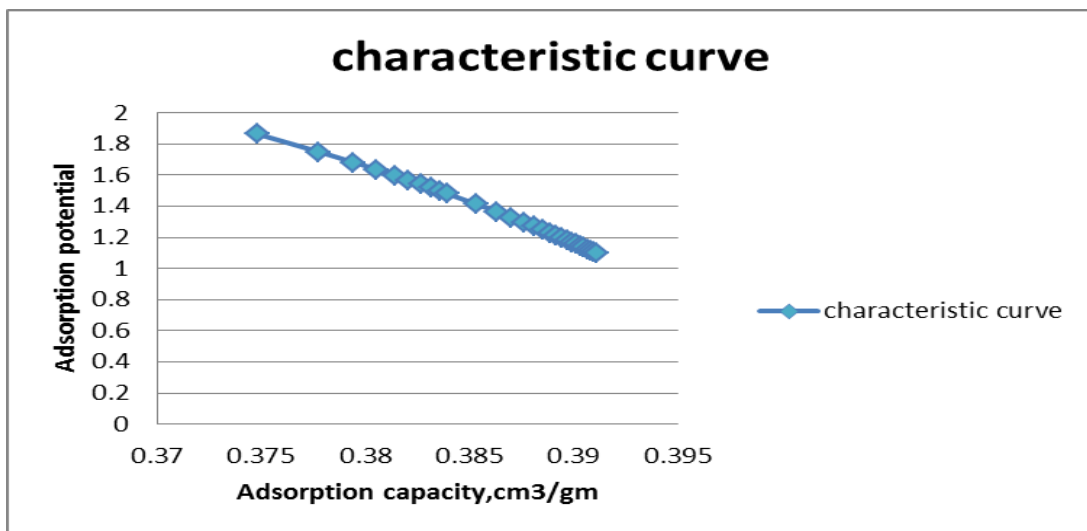


Figure 10 Characteristic Curve of Hydrogen at 20K

Isotherm Generated from D-R equation for Hydrogen:

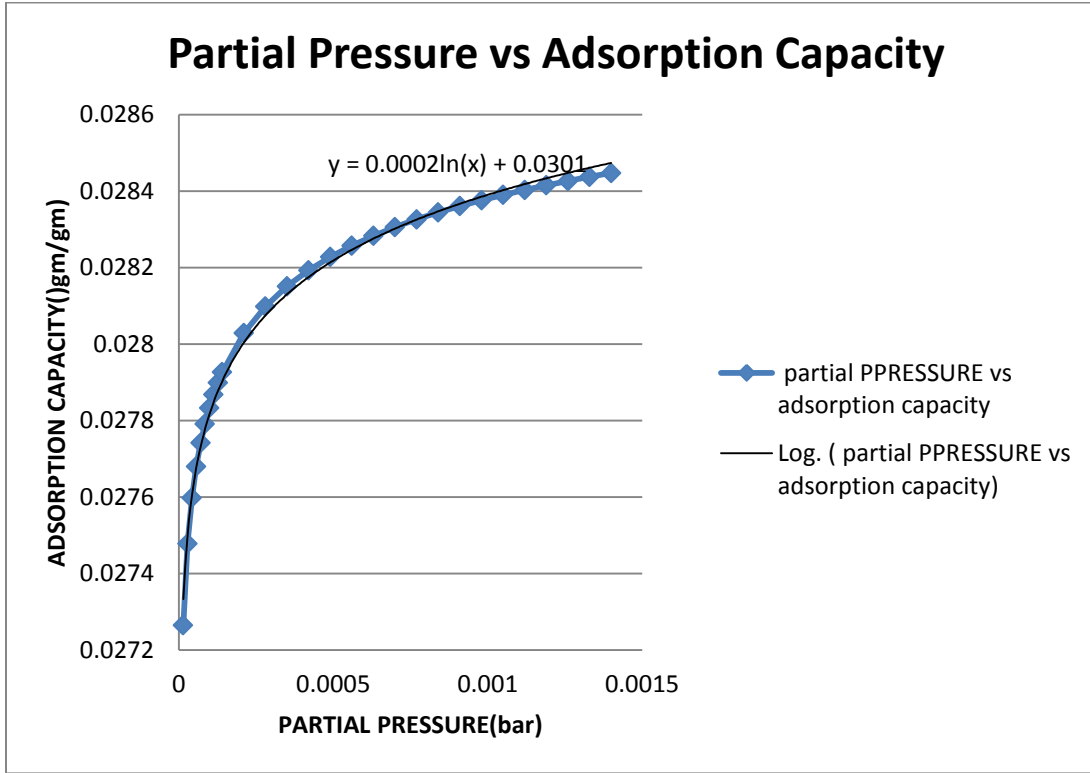


Figure 11 Hydrogen Adsorption Isotherm developed from D-R equation

The required Isotherm obtained at 20K temperature and 14bar pressure for impurity varying from 1PPM to 100PPM.

3.2 ADSORBENT FOR MTZ:

MTZ depends on the bed diameter and hence before MTZ calculation, this assumption is taken and after finding appropriate diameter, MTZ is calculated and then final length of the bed and pressure drop are estimated. For MTZ calculation we need to decide the dimensions of the charcoal used, void fraction and the dimensions for of the bed for the calculation purpose. All these above mentioned factors are decided by the pressure drop optimization. So the next step is the optimization of the pressure drop and selection of different parameters.

3.21 Optimization of the pressure Drop:

For Optimization purpose taking 100% margin over the mass of the charcoal found, hence the new mass is found to be 20 kg. MTZ depends on the bed diameter and hence before MTZ calculation, this assumption is taken and after finding appropriate diameter, MTZ is calculated and then final length of the bed and pressure drop are estimated. For various Lengths to diameter ratios for the bed and varying the void fraction and the charcoal particle diameter pressure drop is calculated using ERGUN equation.

$$M_{ad}=10\text{kg}$$

Taking 100% margin over M_{ad} to get optimum length and diameter for pressure drop

$$M_{ad} = 2 * 10 = 20\text{Kg}$$

$$\rho_{\text{coal}}=550 \text{ kg/m}^3$$

$$V_{\text{coal}}=0.0363636 \text{ m}^3$$

$$D_p=0.002 \text{ m}$$

$$\varepsilon= 0.48 \text{ (Void porosity)}$$

Taking $L/d=2.5$ the dimensions of d and L are

$$d = 0.25763 \text{ m}$$

$$L= 0.644075 \text{ m}$$

$$U_0= 0.057382 \text{ m/sec}$$

$$U_I= 0.119546 \text{ m/sec}$$

$$R_e= 1806.345$$

$$F_p= 1.833041$$

$$\Delta P= 305.526 \text{ Pa}$$

$$= 3 \text{ mbar}$$

From these above calculations it is found that for particle diameter 0.002m and void fraction 0.48 the pressure drop is coming well below the range.

3.3 HENRY CONSTANT (K_H):

Two models have been discussed in the literature survey for the calculation of the mass transfer zone. One of the most important parameter in calculating the MTZ is the HENRY constant. The procedure for Henry constant is described below.

NOTE: In actual practice D-R equation doesn't reduce to Henry's law but the isotherm obtained is having resemblance with Type-1, Langmuir type. At very low pressure the Langmuir isotherm converted to Henry isotherm and there exists a linear relationship between the volume adsorbed and the pressure and the slope of the curve gives the HENRY CONSTANT (K_H).

Henry constant needs to be calculated in dimensionless form, the equation to calculate Henry constant is in the form [5,17,19] $K_{H,CC} = C_{aq}/C_{gas}$

Or in the form of $P = K_H * C$

P = partial pressure of the solute in the gas

K_H = Henry constant

C = concentration of the solute

We tried to find out the Henry constant in dimensionless form by equating the partial pressure and the adsorption capacity. The reason being taking adsorption capacity (gm of H₂/ gm of carbon) is as adsorption happens the concentration of the hydrogen decreases in the gas mixture and it starts increasing in the carbon surface.

As per the sample calculations used:

For 1 PPM impurity

$P = (1 \text{ lit of H}_2 \text{ at 1 bar and 300K} / 10^6 \text{ lit of He at 1 bar and 300K})$

Density of Helium at 300K and 14 bar is 15 times the Density at 20K and 14 bar, hence

At 14 bar and 300K the amount of impurity=15*1

$$=15\text{lit}$$

At 1 bar and 300K the amount will be $=(15*14)/22.4$

$$=9.37 \text{ moles}$$

Partial pressure= $9.37*10^{-6}$ moles of H₂/lit of He

Adsorption capacity at 1ppm(C)= 0.027264865gm of H₂/gm of carbon

$$= 7.438331103 \text{ mol of H}_2/\text{lit of carbon}$$

Using these relation the Isotherm found is

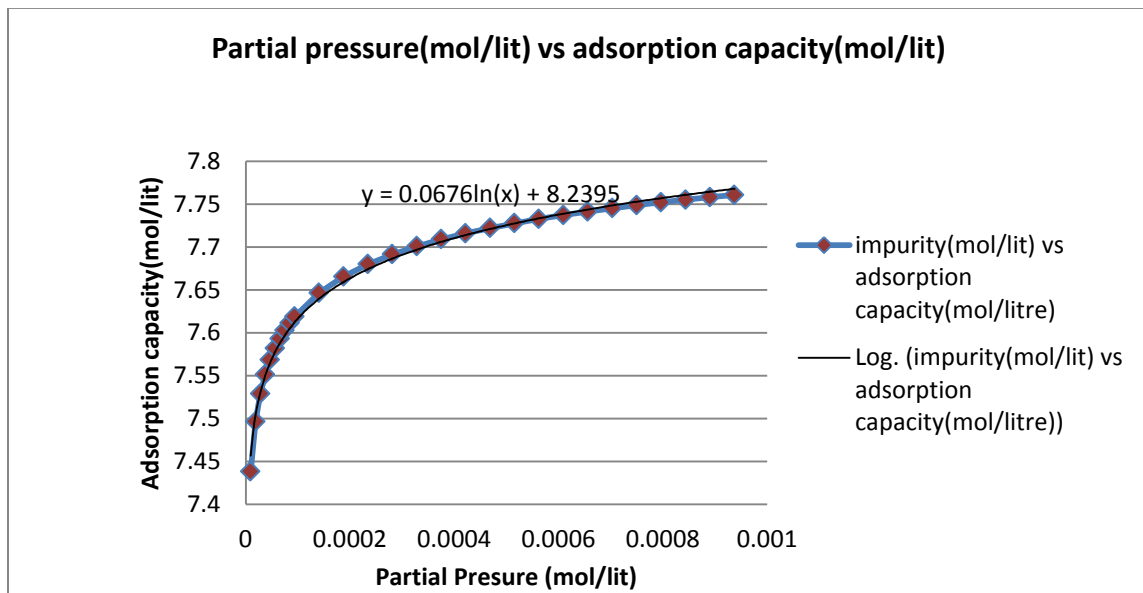


Figure 12 Adsorption Isotherm correlation for Henry constant

From the curve fitting the equation is found to be

$$Y=0.0676 \ln(x)+8.2395$$

The slope of this equation will give the value of Henry Constant. From the above equation the value of Henry constant is found 7210.

Dimensionless Henry constant $K_H= 7210$

3.3.1 Effective Diffusivity Calculation:

For Helium(A) and Hydrogen(B) system[12,19]

$$T=20K$$

$$\sigma_A=2.827 \text{ \AA}$$

$$\sigma_B=2.827 \text{ \AA}$$

$$\sigma_{AB}=2.698 \text{ \AA}$$

$$\epsilon_A=10.22$$

$$\epsilon_B=59.7$$

$$\epsilon_{AB}=24.7$$

$$(kT/\epsilon_{AB})=0.8097$$

$$\Omega_D=f(0.8097)$$

$$=1.612$$

Using above values in equation (17),(18),(16)

$$D_M=8.82*10^{-8} \text{ m}^2/\text{sec}$$

$$D_K=3.06*10^{-7} \text{ m}^2/\text{sec}$$

$$D_e=6.846E-08 \text{ m}^2/\text{sec}$$

3.4 MTZ using Axial Dispersion Model:

$$R_e=1806$$

$$Sc=1.782$$

$$D_e=6.846E-08$$

$$D_z=0.000229$$

$$L=0.64m$$

$d = 0.257\text{m}$

$K_H = 7210$

Time (t) starting from 1 sec and increasing at an interval of 500 seconds

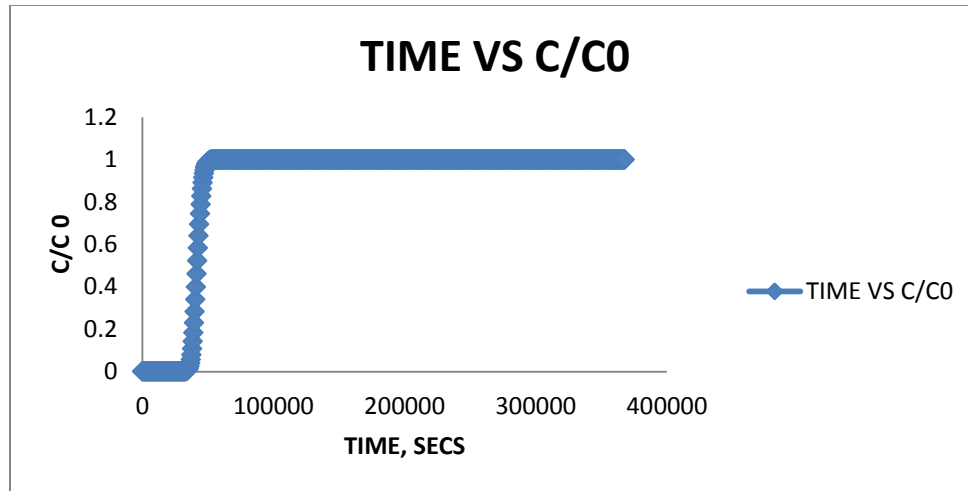


Figure 13 Break Through Curve for Axial Dispersion Model

Break through time (t_B) taken at concentration ratio 0.01 and the saturation time (t_s) taken at concentration ratio 0.9

$t_B = 35001$ secs

$t_s = 46501$ secs

$$L_{MTZ} = L * \frac{t_s - t_B}{t_s}$$

$L_{MTZ} = 0.15$ m

Using axial dispersion model the length of MTZ is found to be 24% of the bed length.

3.5 MTZ using DIMENSIONLESS ROSEN MODEL:

$R_e = 1806$

$Sc = 1.782$

Sh=109.4224

$D_e=6.846E-08$

L=0.64m

d =0.257m

$K_H=7210$

Dimensionless Bed length (V)=7324.822

Dimensionless film resistance (v)=131.7829

Time (t) starting from 1 sec and increasing at an interval of 100 seconds

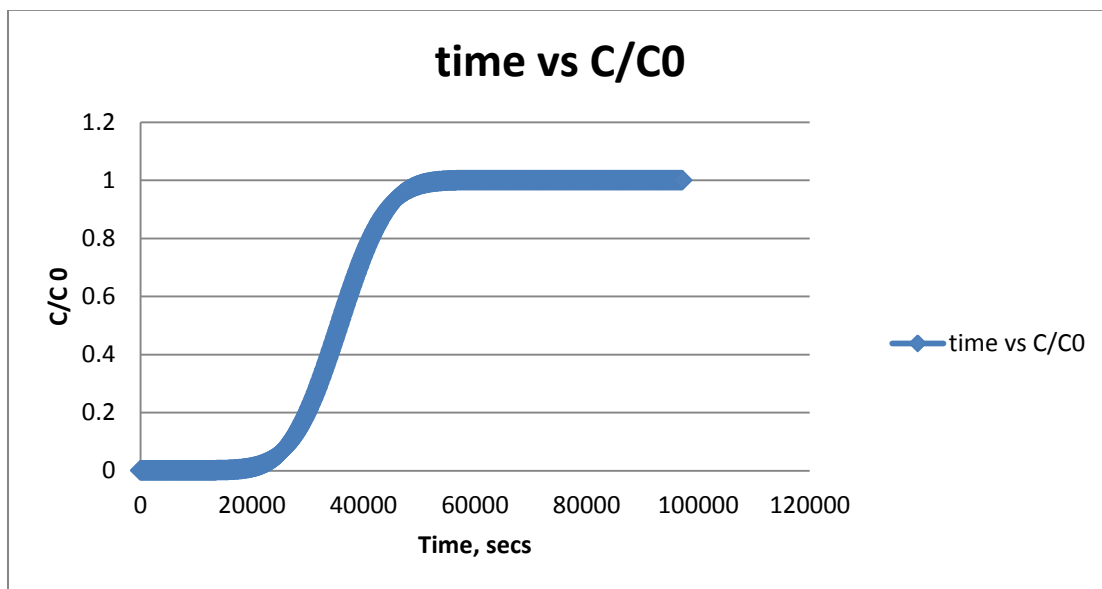


Figure 14 Break through Curve using Rosen Model

$t_B= 24901$ secs

$t_S= 41601$ secs

$$L_{MTZ} = L * \frac{t_S - t_B}{t_S}$$

$L_{MTZ}=0.258$ m

Using the dimensionless Rosen Model MTZ is found to be 40% of the total bed Length.

3.6 FINAL DIMENSIONS OF THE BED AND PRESSURE DROP:

From Rosen Model and Axial Dispersion model, Rosen Model shows the higher percentage of the MTZ length. So for the safe design criteria it's better to take higher percentage of MTZ length, hence final design of the Adsorber Bed will be based on ROSEN MODEL.

For final Length of the bed to be calculated using the equation below

$$L_{TOTAL} = L_{SAT} + 0.4L_{SAT} + \%L_{MTZ} \text{ of the } L_{sat}$$

From D-R equation the mass of adsorbent is found to be 10kg

Taking diameter $d=0.257\text{m}$ the **SATURATION LENGTH** of the bed is found to be 0.35m.

$$\begin{aligned} L_{TOTAL} &= 0.35 + 0.4 * 0.35 + 0.4 * 0.35 \\ &= 0.63 \text{ m} \end{aligned}$$

According to ISO Standardization taking the vessel diameter having nominal diameter $d_N=0.250\text{m}$ and Schedule 10 pipe size having

$$d_o = 0.273 \text{ m}$$

$$d_{in} = 0.264 \text{ m}$$

Using these above mentioned dimensions the mass of charcoal required for adsorber bed is found to be 19 kg.

The pressure drop for the dimension found is 2.72 mbar.

3.7 STRESS ANALYSIS OF THE DESIGNED PURIFIER BED IN ANSYS:

Process Parameters:

Table 2 Process Parameters for Stress Analysis of Purifier bed

Length of Cylinder	0.63m
ID of Cylinder	0.264m
OD of Cylinder	0.273m
Hemispherical Dome Diameter	0.132m
HP Line Diameter	2''
Charcoal Pipe Diameter	1''
Inside Pressure	14 bar
Outside pressure	Vacuum Condition

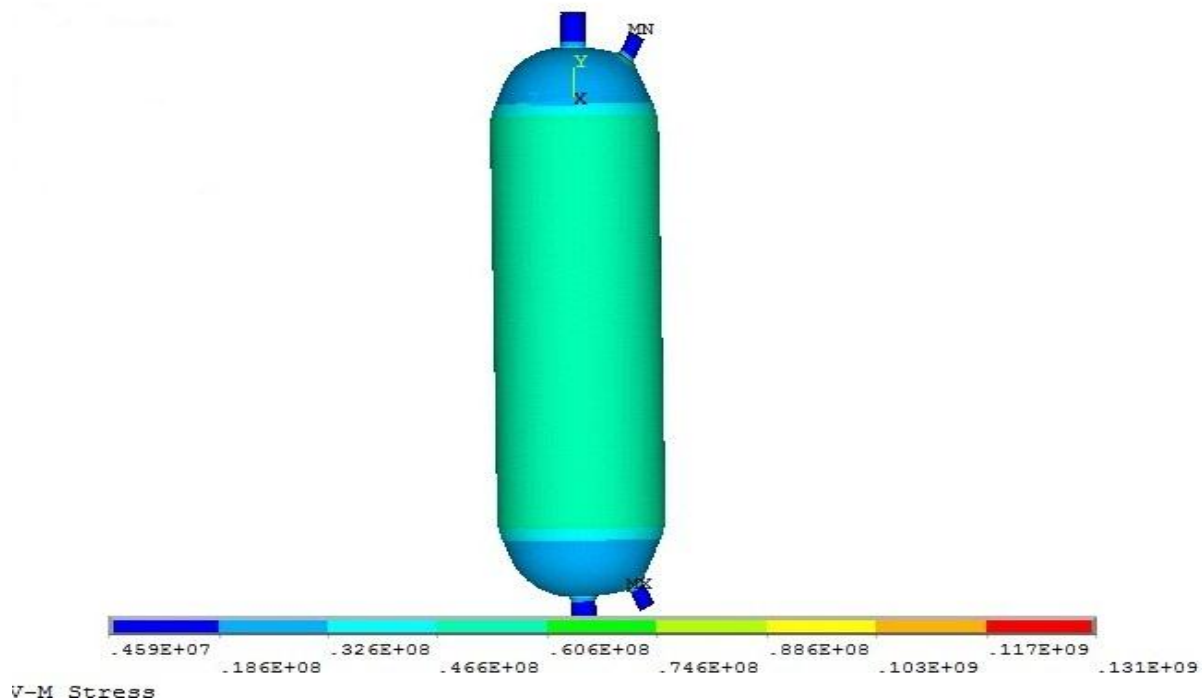


Figure 15 structural analysis of the designed purifier bed in Ansys

Stress analysis is performed in Ansys using the parameters tabulated above. The stress distribution is uniform throughout the cylindrical shell. From stress point of view the design is found safe.

PRESSURE DROP CALCULATION FOR FILTER CATRIDGE

Filter cartridge is a circular tube like structure containing screens for purifying the helium stream. After the Helium stream is purified in the adsorption due to high pressure and very low temperature some of the charcoal granule gets dusted with size varying from 10 to 30 micron which comes in the high pressure line leaving the purifier bed. Charcoal dusts coming in the high pressure line can cause blockages in the pipelines leading to huge pressure drop and inefficient liquefaction. To contain these small particles metallic wire mesh screens of 30micron size used with no of screens varying from 10 to 50.

Table 3 PROCESS PARAMETERS FOR FILTER CARTRIDGE Design

Screen width(1layer)	0.00003m
Wire diameter	0.00003m
Inner diameter of filter	0.08m
Outer diameter of casing	0.161m
Connecting pipe Diameter	0.027m
No of screen	10
Length of the cartridge	0.175m
Void fraction in Screen	0.3

In case of designing of the filter cartridge ERGUN equation is used

The expression of ERGUN equation for the calculation of pressure drop across a metallic screen is given by

$$Re_{Erg} = \frac{\rho V_s^6}{\mu}$$

$$fr = \frac{\alpha}{Re} + \beta$$

$$\Delta P = \frac{fr \rho V_s^2 B (1-\epsilon) a}{6 \epsilon^3}$$

Taking $\epsilon=0.3$

$$\alpha=150(1-\epsilon)$$

$$\beta=1.75$$

$$\text{Screen width (B)} = 30 \times 10^{-6} \text{ m}$$

$$\text{Wire diameter (d)} = 30 \times 10^{-6} \text{ m}$$

$$\text{Inner diameter of filter (D)} = 0.08 \text{ m}$$

$$\text{Outer diameter of casing (D}_0\text{)} = 0.17 \text{ m}$$

$$\text{Connecting pipe Diameter (D}_p\text{)} = 0.027 \text{ m}$$

$$\text{Length of the cartridge (L)} = 0.175 \text{ m}$$

$$a = 4/d$$

$$= 1.33 \times 10^5$$

$$\text{Volume flow rate of Helium} = 0.003 \text{ m}^3/\text{sec}$$

$$\text{Velocity across Screen (V}_s\text{)} = \frac{Q}{\pi DL}$$

$$= 0.06820926 \text{ m/sec}$$

$$\text{Re}_{\text{Erg}} = 25.1219494$$

$$\text{Fr} = 5.92961196$$

For single screen the pressure drop is found to be 15.9401484 Pascal. For 10 screens the pressure drop is 159.4 pascals

Inlet Pressure loss is equal to outlet pressure loss as the diameter of the connecting pipe is same

$$\text{Inlet pressure loss } (\Delta p) = 458.895787 \text{ pa}$$

$$\text{Outlet pressure loss } (\Delta p) = 458.895787 \text{ pa}$$

$$\text{Pressure loss at the annular space} = 0.1697653 \text{ pa}$$

$$\Delta P_{\text{Total}} = 10773.63 \text{ pa}$$

The total pressure drop inside the filter cartridge is found to be 10.77 mbars.

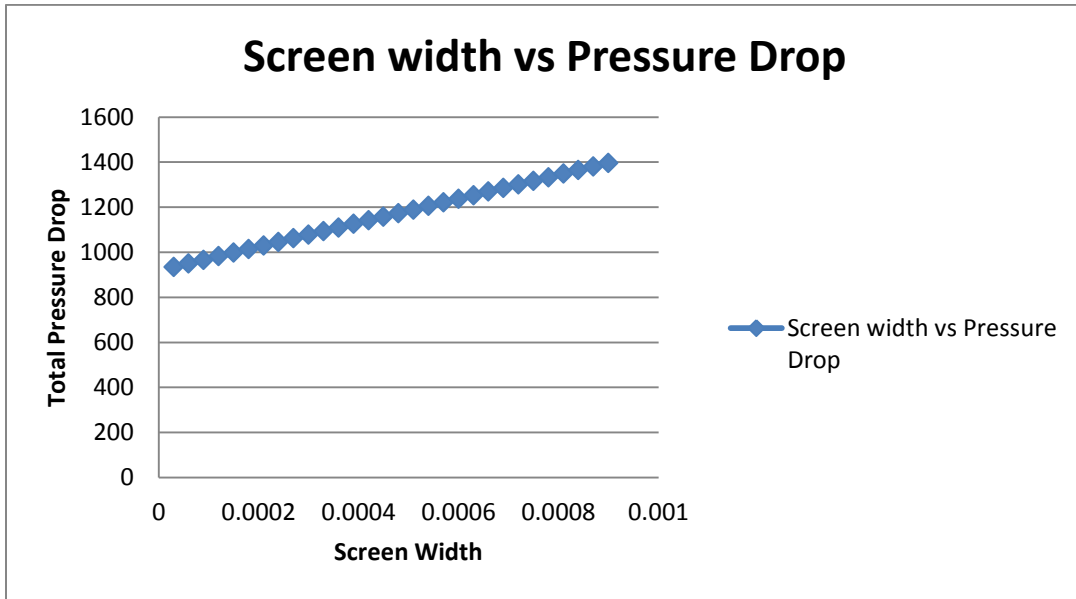


Figure 16 Pressure Drop vs. Screen Width for Filter cartridge

With increase in the screen width (i.e. no of screens) the total pressure drop increases linearly as the values of entry and exit pressure drop are same.

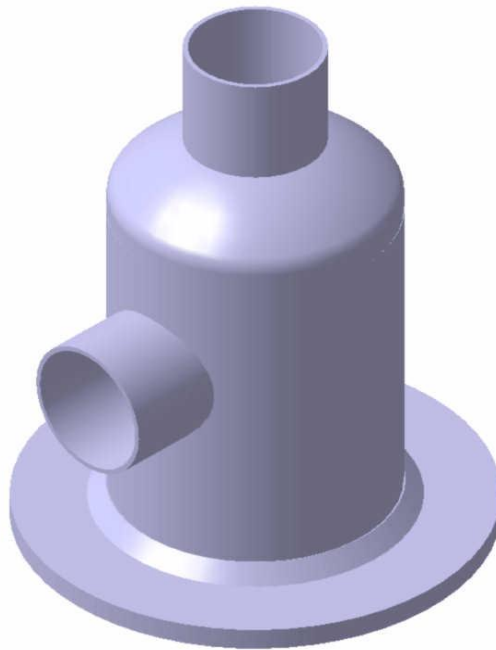


Figure 17 3-D drawing Outer Casing of the Filter Cartridge

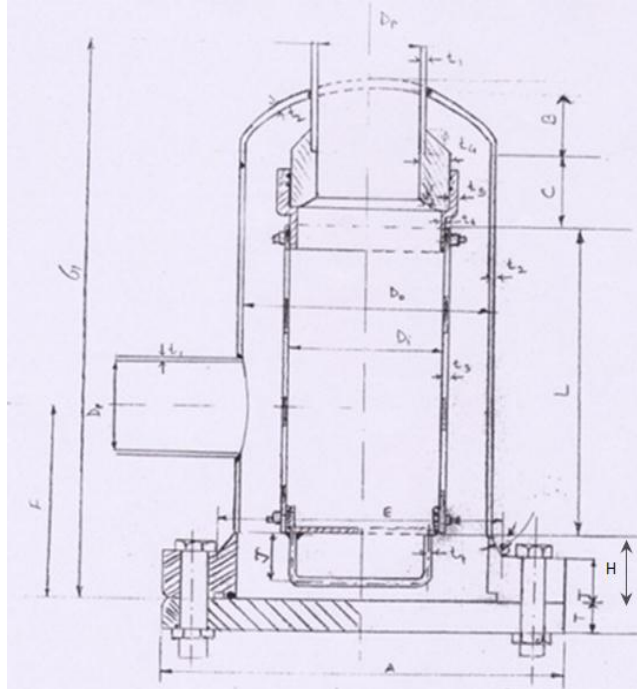


Figure 18 2-D drawing of inner design of the filter cartridge

Table 4 Internal design and dimensions of the Filter cartridge

D_i	80
D_0	170
D_p	54
L	175
A	279.4
E	192.08
T	13.49
t_1	3.048
t_2	4.191
t_3	0.3
t_4	8.5
t_5	4.25
t_6	2.2
B	68.26
H	88.9
C	30
F	127
G	374.65
J	60
θ	37.5°
α	45°

φ	45 ⁰
No of Holes	8
Diameter of Holes	22.22
Diameters of Bolts	19.05
Bolt circle	241.3

The dimensions of the filter cartridge are tabulated above. The dimensions of the flange design are as per the loading conditions [18].

RESULTS AND DISCUSSION

5.1 DIMENSIONS OF THE PURIFIER BED:

The final length of the cylinder is found to be 0.63m and the inner diameter of the cylinder is 0.264m as per ISO standard. The amount of adsorbent required to contain the impurity is found to be 19kg. The pressure drop for these above mentioned dimensions with particle diameter 0.002m and void fraction 0.48 the pressure drop in the purifier bed is found to be 2.72 mbar. A 2-D model in Catia is drawn based on the above mentioned dimensions. In this 2-D model a high temperature gas line is also shown which will be used for Purging/Regeneration operations of the charcoal. The adsorbent used for Purification purpose is Coconut shell based charcoal which is easily available in Indian Market and low cost than other charcoals available.

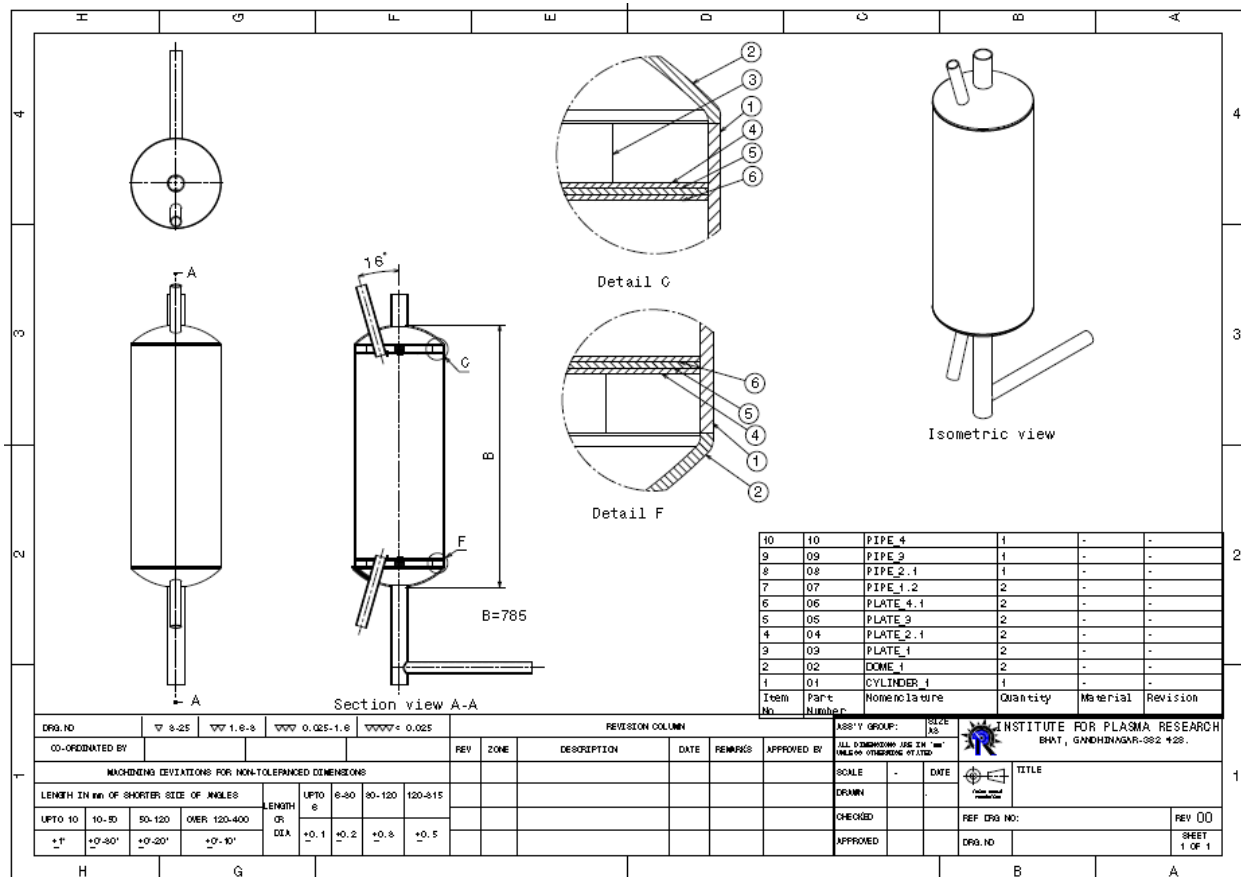


Figure 19 2-D Drawing of 20K Purifier Bed

5.2 PRESSURE DROP IN PURIFIER BED:

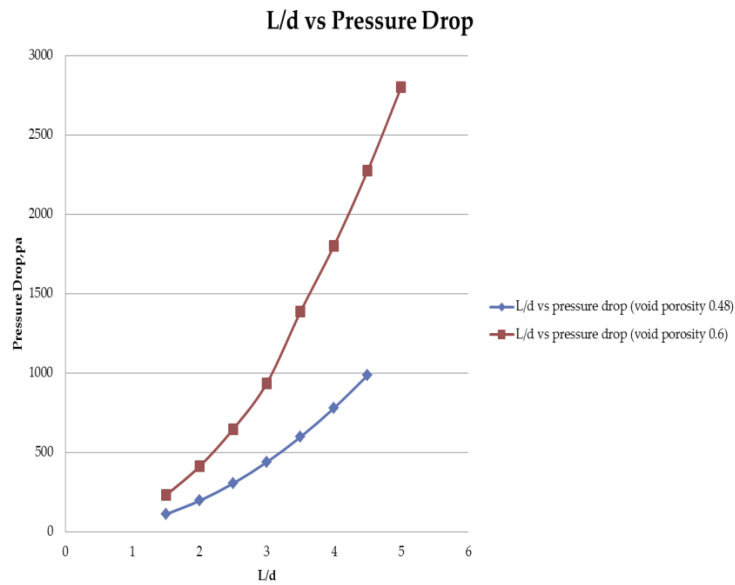


Figure 20 L/d vs. Pressure Drop varying the Void Porosity

Keeping the particle diameter constant and changing the void porosity from 0.48 to 0.6 it shows that, Pressure drop across the bed decreases as the void porosity increases.

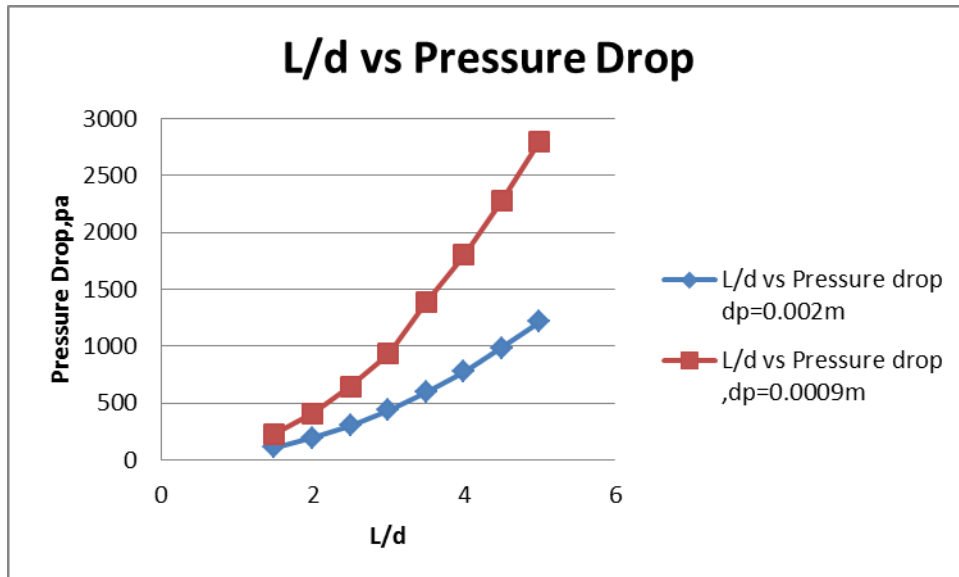


Figure 21 L/d vs. Pressure Drop varying the Particle diameter keeping constant void porosity

Keeping the void porosity constant at 0.48 if the particle diameter decreases, the pressure drop increases.

5.3 Mass Transfer Zone:

5.3.1 Independency of Henry constant for calculation for the MTZ:

5.3.1.1 ROSEN MODEL:

The breakthrough curves obtained for Rosen Model with different K_H values are plotted, keeping all the other parameters constant. It is found that in both the cases the percentage change in the length of MTZ remains constant. Henry constant has no effect on the change of length of MTZ.

Table 5 Independency of Henry constant

Henry Constant	MTZ % Length
80.5	0.41
288.42	0.397
721	0.41
7210	0.39999
32032	0.402

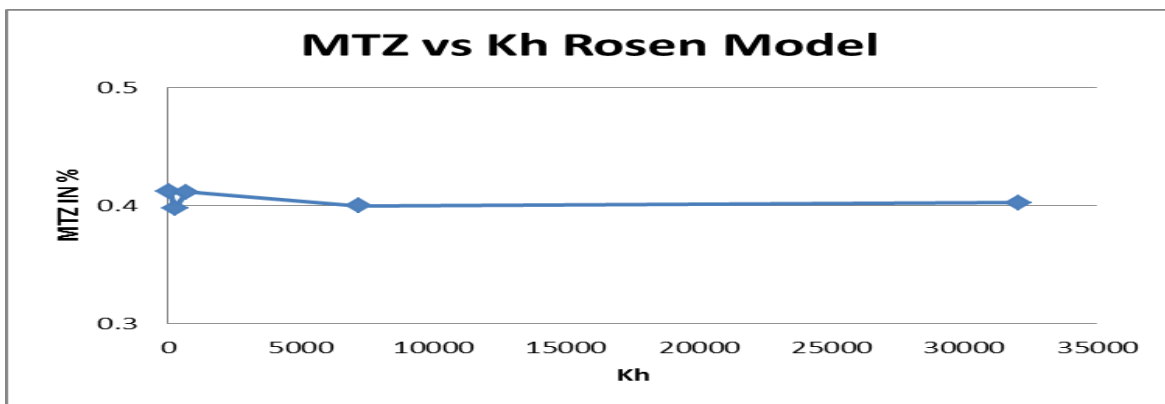


Figure 22 MTZ vs. KH for Rosen Model

In the table shown above the Henry constant value is calculated for different impurity levels. The corresponding MTZ length is calculated and it is found that with change in the K_H has no effect on the MTZ length but with increase in K_H saturation tie increases.

5.3.1.2 Axial Dispersion Model:

In axial dispersion Model also the change in the value of Henry constant is having no change in the MTZ length. Two curves is shown for different Henry constant value.

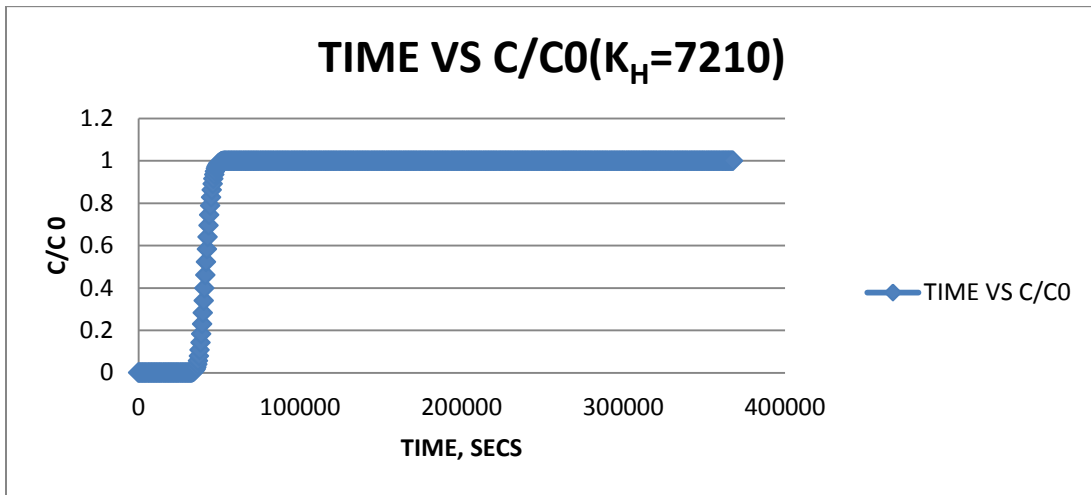


Figure 23 MTZ vs. K_H for ($K_H=7210$)

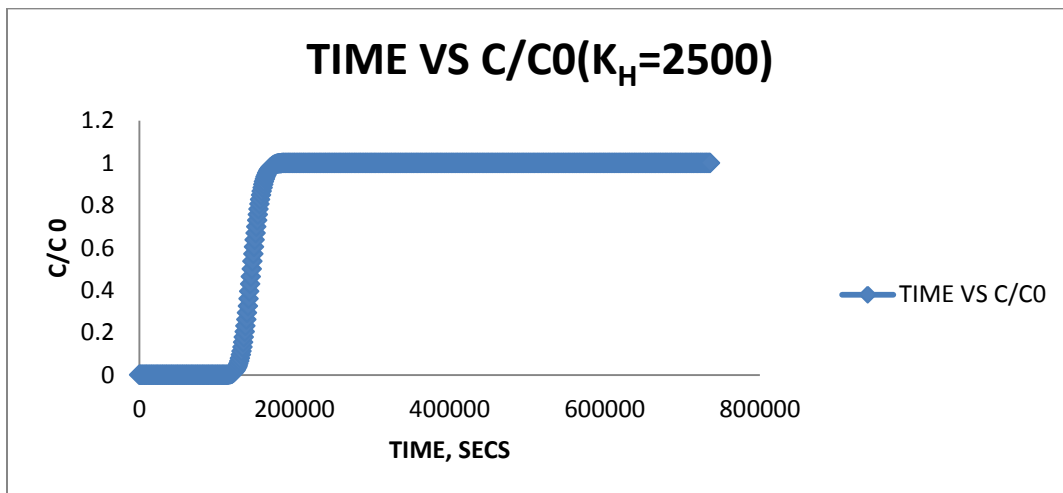


Figure 24 MTZ vs. K_H for ($K_H=2500$)

In both curves shown above the MTZ percentage remains constant irrespective of HENRY CONSTANT and MTZ length percentage is coming 24% in both the cases. Below some detailed analysis is shown based on with keeping Henry constant same and varying other parameters like particle diameter and interstitial velocity.

5.4 MTZ Variation with changing Different Parameters for ROSEN

MODEL:

Time vs Concentration ratio with changing Interstitial Velocity:

Table 6 variation of MTZ with interstitial velocity

Interstitiaal Velocity(U_I)	MTZ(% Change)
0.119546	0.40
0.208333	43.38
0.416667	47.15
0.625	49.31
0.833333	50.71

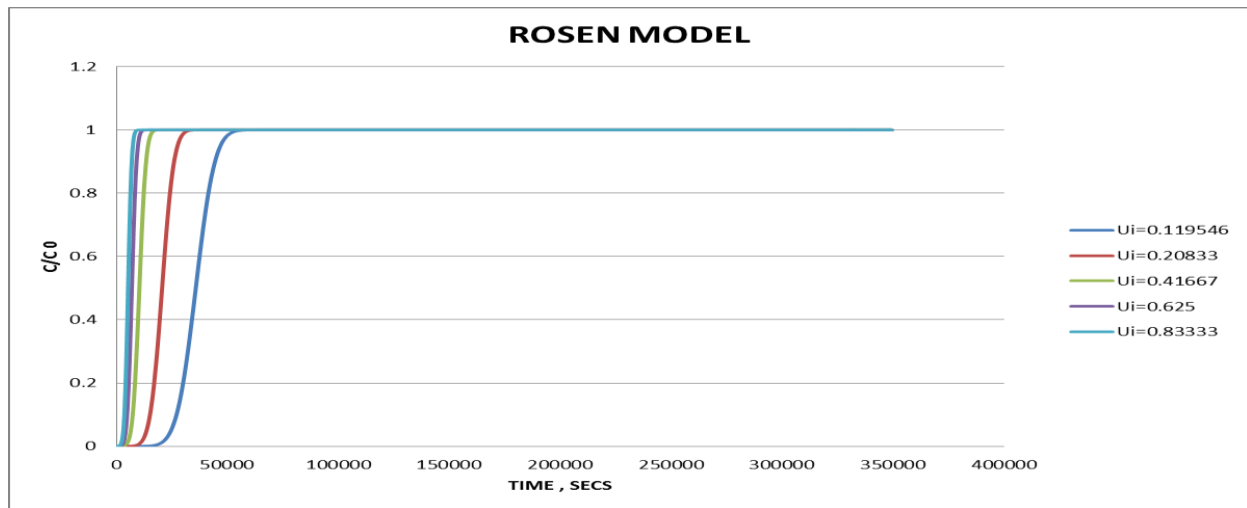


Figure 25 Time vs Concentration ratio with changing Interstitial Velocity for Rosen Model

Keeping the Henry constant same as the interstitial velocity increases the MTZ length in percentage increases, which is undesirable. The interstitial velocity needs to as low as possible.

Time vs Concentration ratio with changing the Particle diameter:

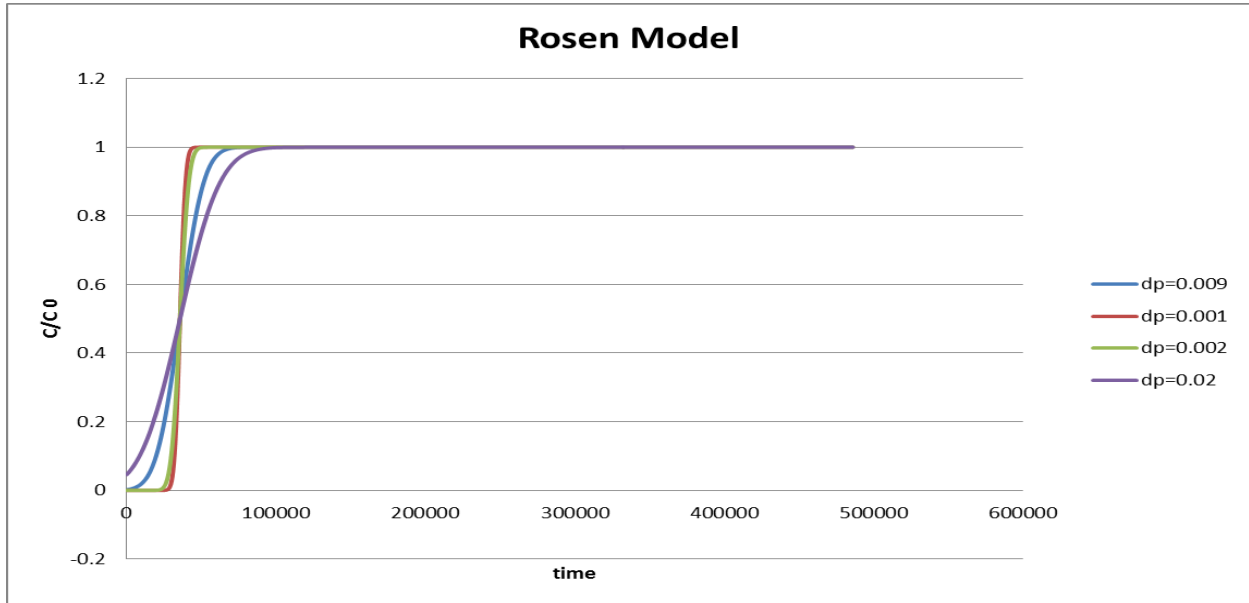


Figure 26 Time vs Concentration ratio with changing the Particle diameter

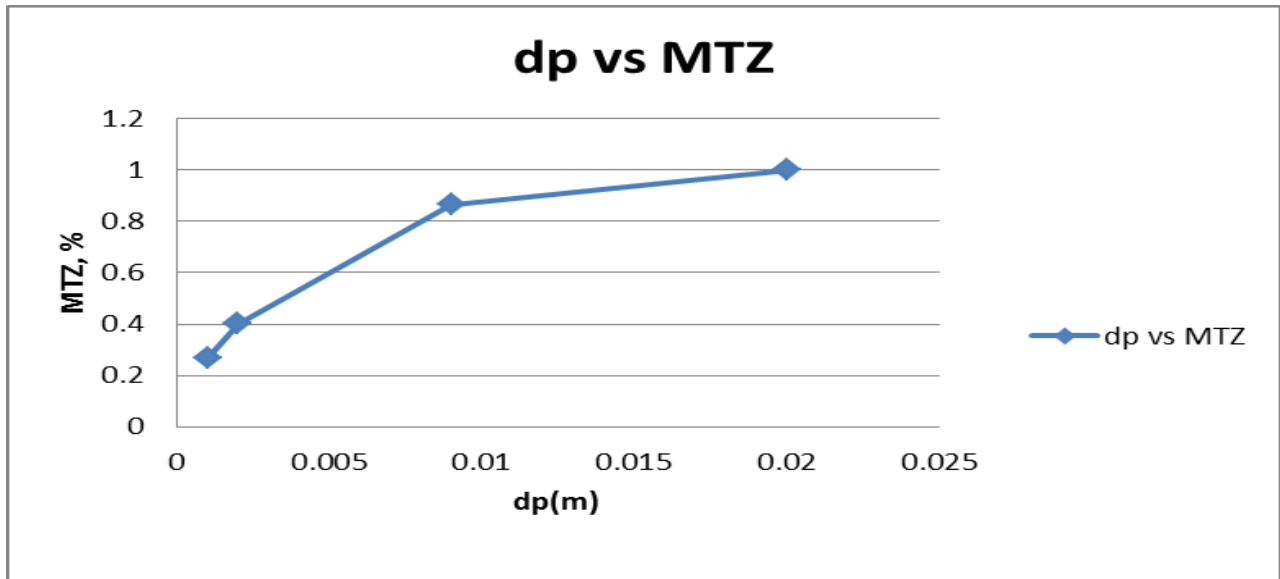


Figure 27 Particle Diameter(meters) vs. MTZ % in Rosen Model

As particle diameter increases the value of percentage change in MTZ increases, hence increases the length of unused bed and causes inefficient adsorption.

5.5 PRESSURE DROP VARIATIONS IN THE SCREEN:

Pressure Drop Variation with porosity:

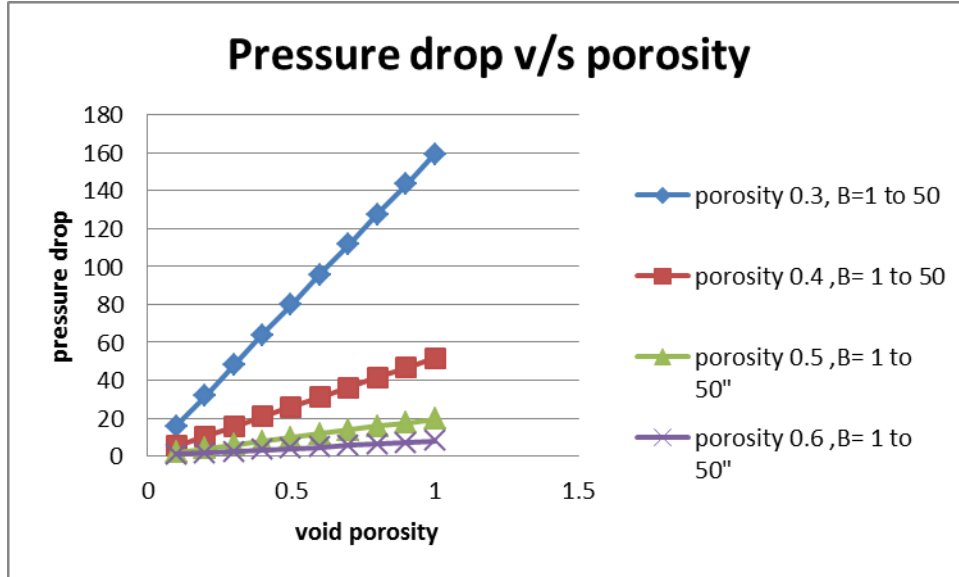


Figure 28 Pressure Drop Variation with porosity for Filter Screen

In the filter cartridge as the void porosity increases the pressure drop decreases but it also increases the chances of contamination in the helium stream so the desirable porosity is taken as 0.3.

Pressure Drop Variation with Screen Width:

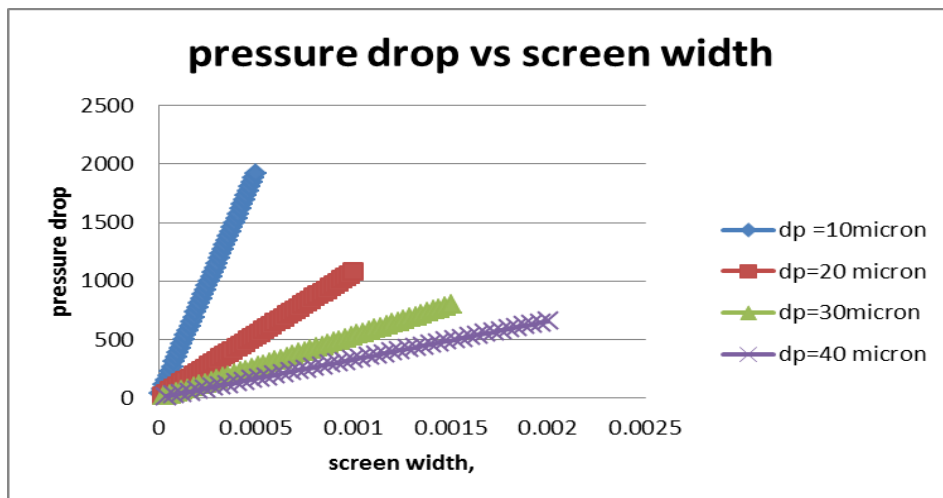


Figure 29 Pressure Drop Variation with Screen Width

In the above graph it is shown that as the screen width decreases the pressure drop increases, i.e. for small wire diameter the pressure drop is higher and can go up to 25mbar only for filter cartridge which is undesirable. So the optimum wire diameter used here is 30 micron.

CONCLUSION:

Adsorbent mass required for Helium purification is 19 kg, the container of the vessel is also designed to have diameter 0.264 m and height 0.63m Pressure drop is calculated for sample of carbons and found to be 2.72 mbar. Also a filter cartridge is designed, which can filter charcoal particles size less than 30 micron which has pressure drop of 10.77 mbar. The total pressure drop for the system is 13.5 mbar well within the allowed value of 50 mbar. Mass transfer zone is calculated using two analytical models (Rosen and Axial dispersion model) and with different Henry constants. MTZ length found to be different from two different models, but in each model, MTZ length remains nearly constant for different variation of Henry constants. So we conclude that MTZ length is independent of Henry constant. The variation of MTZ length is shown with changing interstitial velocity and the particle diameter of the charcoal. It is found that as the interstitial velocity increases the % MTZ length increases which is not desirable. Hence interstitial velocity should be as low as possible. As the particle diameter of the charcoal sample increases the % MTZ length increases, so while choosing the charcoal it should be taken into consideration.

FUTURE SCOPE:

1. Experimental procedure can be established to find out the actual MTZ length. And the MTZ length found can be compared with two different models described above.
2. Experimental testing can be done on different charcoal sample available in the market Indian and Overseas.
3. Flow patterns inside the packed bed can be predicted using FLUENT.

REFERENCES:

- [1]Purer, A., Stroud, L., & Meyer, T. O. (1965). Simple Technique for the Ultrapurification of Helium. In *Advances in Cryogenic Engineering* (pp. 398-401). Springer US.
- [2]Kidnay, A. J., & Hiza, M. J. (1967). High pressure adsorption isotherms of neon, hydrogen, and helium at 76 K. In *Advances in Cryogenic Engineering* (pp. 730-740). Springer US.
- [3]Kidnay, A. J., Hiza, M. J., & Dickson, P. F. (1968). the Adsorption Isotherms of Methane, Nitrogen, Hydrogen and their mixtures on Charcoal at 76 K. *Advanced in Cryogenic Engineering. Vol, 13*, 400.
- [4]Wang, Q., & Johnson, J. K. (1998). Hydrogen adsorption on graphite and in carbon slit pores from path integral simulations. *Molecular physics*, 95(2), 299-309.
- [5]McCabe, W. L., Smith, J. C., & Harriott, P. (1993). *Unit operations of chemical engineering* (Vol. 5). New York: McGraw-Hill.
- [6]Barron, R. F. (1985). Cryogenic systems. *Monographs on Cryogenics, New York: Oxford University Press, and Oxford: Clarendon Press, 1985, 2nd ed.*,
- [7]Hutson, N. D., & Yang, R. T. (1997). Theoretical basis for the Dubinin-Radushkevitch (DR) adsorption isotherm equation. *Adsorption*, 3(3), 189-195.
- [8]Wood, G. O. (2001). Affinity coefficients of the Polanyi/Dubinin adsorption isotherm equations: A review with compilations and correlations. *Carbon*, 39(3), 343-356.
- [9] Stoeckli, H. F., Kraehenbuehl, F., Ballerini, L., & De Bernardini, S. (1989). Recent developments in the Dubinin equation. *Carbon*, 27(1), 125-128.
- [10]Yang, R. T. (1986). Gas separation by adsorption processes.
- [11]Perry, R. H., Green, D. W., & Maloney, J. O. (1984). Perry's chemical engineer's handbook. In *Perry's chemical engineer's handbook*. McGraw-Hill Book.

[12]Treybal, R. E., & Treybal Robert, E. (1968). *Mass-transfer operations* (Vol. 3). New York: McGraw-Hill.

[13]www.norit.com

[14]Subramanian, R. S. (2004). Flow through Packed Beds and Fluidized Beds. *Clarkson University*, [cited February 2007], <http://www.clarkson.edu/subramanian/ch301/notes/packfluidbed.pdf>.

[15]Fischer, A., & Gerstmann, J. (2013). Flow Resistance of Metallic Screens in Liquid, Gaseous and Cryogenic Flow.

[16]Dubinin, M. M. (1983). Microporous structures and absorption properties of carbonaceous adsorbents. *Carbon*, 21(4), 359-366.

[17] http://en.wikipedia.org/wiki/Henry's_law

[18]Brownell, L. E., & Young, E. H. (1959). *Equipment Design*. John Wiley & Sons.

[19] Ruthven, D.M. (1984) *Principles of adsorption and adsorption processes*. Wiley, New York